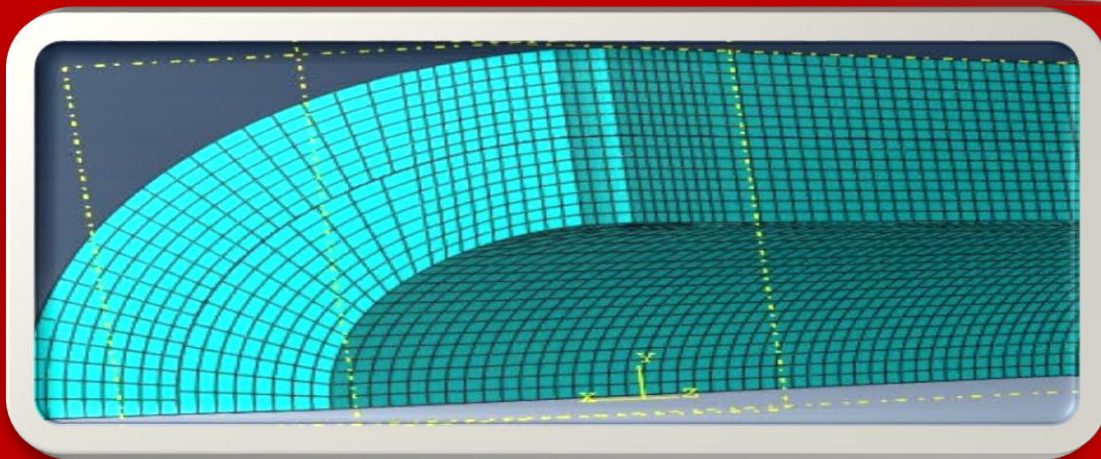
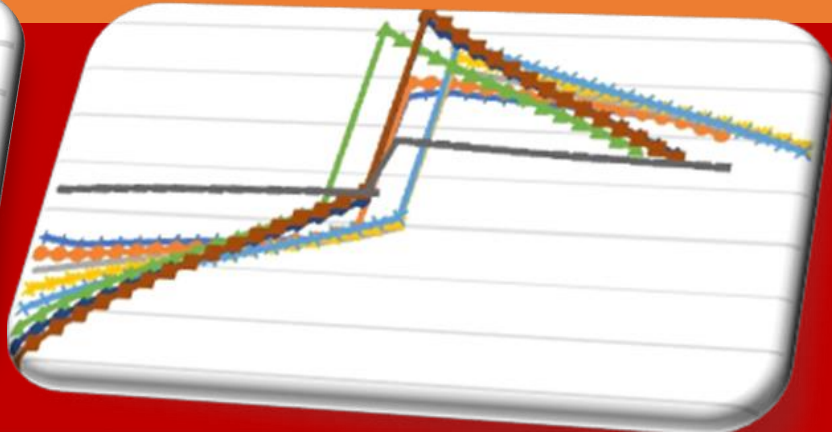
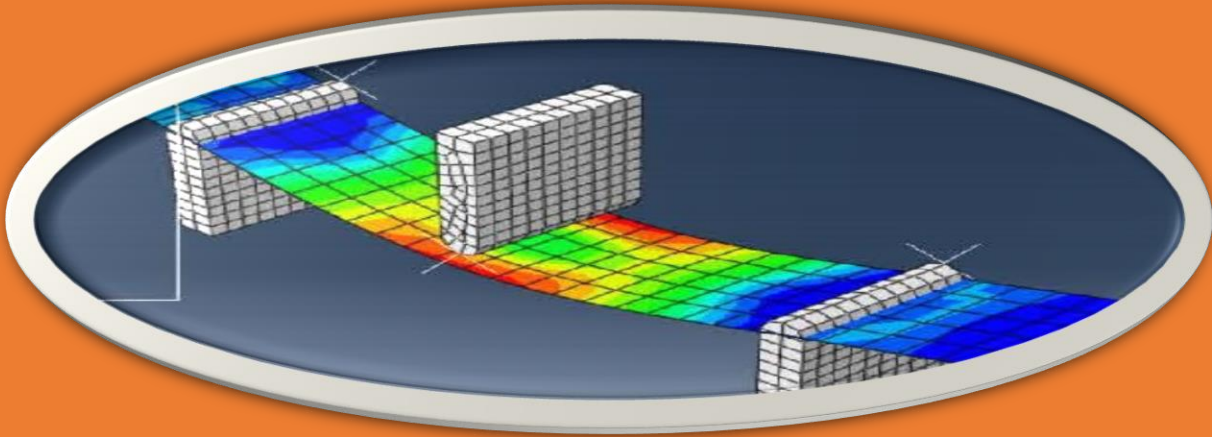




African Journal of Engineering Research and Innovation

AJERI Vol 2. No. 4. 2024



The Institution of Engineers of Kenya

In partnership with



AJERI

African Journal of Engineering in Research and Innovation

ISSN: 2957- 7780

Volume 2. No 4. 2024

IEK

Published by:

The Institution of Engineers of Kenya

P.O Box 41346- 00100

Nairobi Kenya

Tel: +254 (20) 2729326, 0721 729363, (020) 2716922

Email: editor@iekenya.org

Website: www.iekenya.org

African Journal of Engineering Research and Innovation (AJERI), is published by **The Institution of Engineers of Kenya, IEK**, as an international forum for publication of high-quality papers in all areas of Engineering

CONTENTS

Pages

Correlation between material properties and distress features in gravel roads..... 1

F. C. Korir, S. N. Osano, S. K. Mwea

Evaluation of the Effectiveness of Rice Straw Fibres on Expanded Polystyrene Lightweight Concrete..... 23

W. O. Mocha, S. W. Mumanya, S. O. Abuodha

Improving the municipal solid waste storage system for islands with popular tourist sites and remote locations using adept storage systems with ventilation systems 37

J. N. Mativo, M. G. Kim, B. O. Alunda

Wellhead Steam Turbine Retrofit 51

L. Muloli, P. Chege, C. Maiko, A. Wamwaki

Informal Settlements challenges implications on the technical solution design for electricity access 61

O. A. A. Ezzaldeen, A. Muumbo

Evaluating the Effectiveness of Pumice on Polyvinyl Chloride (PVC)-Treated Red Coffee Soil for Subbase Construction..... 69

C. D. Anyango, M. W. Kibe, J. N. Thuo

Correlation between material properties and distress features in gravel roads.

F. C. Korir*, S. N. Osano, S. K. Mwea

University of Nairobi, Kenya.

*Corresponding author: korirfc@gmail.com

Article History

Submission Date: 2nd October 2024

Acceptance Date: 6th November 2024

Publication Date: 31st December 2024

Abstract

Road transport is a catalyst in the social and economic development process and is key in the provision of key amenities. In Bomet County, Kenya, over 1500kms of roads have been opened up and graveled since 2015. Despite this investment, the roads continue to deteriorate drastically under two years after completion. This paper investigated the rapid deterioration by correlating the distress features in gravel roads post-maintenance vis-a-vis material properties of gravel used. The general objective was to establish the effect of material properties on the rate of road deterioration. Five roads, one in each sub-county and their corresponding borrow pits were sampled. Gravel road deterioration was established through visual survey of the surface condition using the Unpaved Road Condition Index (URCI) method. The distress features measured were rutting, corrugations, potholes, loose aggregates, inadequate drainage, improper road formation and dust. The corresponding borrow pit material used was tested in accordance with BS 1377: 1990 specifications. Three samples were collected in the corresponding borrow pits, per road, per sub-county. A total of fifteen gravel samples were collected and transported to the materials laboratory for testing. The tests conducted were; Particle size distribution, Atterberg limits, Compaction test, California Bearing Ratio (CBR) and swell at 4 days soak, on specimen molded at Optimum Moisture Content (OMC) at 3 levels of compaction, 90%, 95% and 100% Maximum Dry Density (MDD). The various distress features identified were correlated with the initial material properties of the gravel used. The study established a correlation of 0.9 and 0.8 between the Plasticity Index and distresses loose aggregate and potholes respectively. CBR was found to primarily correlate with rutting by 0.5. The percentage of fines in gravel correlated with distress features loose aggregates, corrugations and potholes by 0.5, 0.8 and 0.6 respectively. The MDD correlated with ruts and corrugations by 0.7 and 0.6. The OMC correlated with corrugations and potholes by 0.8 and 0.7. These findings indicate that the material used for road construction plays a role in its deterioration rate. During design, the incorporation of the findings leads to quality, sustainable

designs while together with proper workmanship, meteorological and geographical data about the area, more durable gravel roads can be guaranteed during construction.

Key abbreviations: Gravel road deterioration, Gravel Material Properties, Material Testing, Unpaved Road Condition Index, Gravel roads

1. Introduction

1.1. Introduction

Gravel roads are constructed and maintained annually in Sub Saharan Africa, in particular rural Kenya. Over 500kms are constructed annually in Bomet County, Rift Valley. This development has since improved transport, however, the state of the road infrastructure in rural Kenya is still wanting as roads continue to deteriorate faster than they are maintained. This deterioration in general negates the positive impact brought upon by annual maintenance. Road deterioration is a factor of climate of the area, traffic, road drainage and properties of material used (Alzubaidi & Magnusson, 2002). The paper sought to isolate and investigate how the material properties of gravel used in road maintenance correlate with the distress features observed in the various roads sampled in Bomet County, Kenya. The roads sampled were last maintained in 2019, and the study conducted four years later. The distress features indicate the rate of deterioration of the roads. The findings will inform the selection of borrow pits and in turn improve the quality of road infrastructure constructed.

1.2. Objectives

The overall objective was to establish the correlation between borrow-pit materials properties with the distress features developed in gravel roads constructed of the same. The paper compared each property with the distress features to establish whether it contributes to their occurrence. Material properties correlated include plasticity index, percentage fines, optimum moisture content, and maximum dry density. The distress parameters directly correlated include; potholes, rutting, presence of loose aggregates and corrugations.

1.3. Deterioration of Gravel Roads

Deterioration of roads is contributed to by several factors including; quality of gravel material used, workmanship, weather conditions and traffic volumes. Adverse weather conditions; specifically wind and rain effectuates the loss of gravel on a gravel road (Sunley, 1996). Distress features require prompt maintenance to avoid further deterioration resulting in road failure.

The major cause of wear of the road is traffic (Alzubaidi, 1999). Traffic causes erosion of the gravel in two ways. The first way is due to the wave disturbance caused and also abrasion

due to the friction and torque developed by the driving wheel. Under the vehicle loads, the particles on the road surface experience high stresses that leads to displacement. This displacement of particles is transmitted to the lower layers of the road and ultimately leads to pavement deflection (Jones , Robinson , & Snaith, 1984).

The particles also rub against one another and are ground, eventually the larger particles become smaller. These are dislodged by the vehicle tailwind and are thrown in the air and others displaced by the vehicles at high speed to the side of the road (Da Silva, Ribeiro, Furlan, & Fabbri, 2021). The more it occurs, the more fines are generated and the road becomes easily dented and rutted.

Different seasons affect gravel roads differently. During the rainy season, gravel absorbs the water and hence reducing the bearing capacity. When it's hot and dry, the road surface and subsequent layers dry up and cohesion decreases significantly. Dust is then generated, which when easily displaced leads to ruts and dents along the carriageway (Skorseth, 2000).

Abrasion occurs during grading of the road. The grader blade grazes, crushes and cuts into the gravel surface. Abrasion is highest in dry conditions, and lowest during wet conditions. Overall, the abrasion caused by a grader is way less compared to that caused by traffic loads (Federal Highways Authority, 2015).

1.4. Road distress features

Fines dispersed in the air is dust which therefore means that the larger and medium sized particles in the road structure remain unbound. This dust defect causes other distresses like compaction of the road fill material and lowered cohesion (Jones, 1984). Ravelling is the loss of larger gravel particles. The loss occurs when particles get displaced by traffic after fine particles have been lost as a result of erosion and carried away as dust (Yellow Rivers Watershed Management Authority, 2000).

Slipperiness occurs when the road has more fines than coarse particles on the road surface. Coarse aggregates get crushed during dry seasons under vehicular loading causing disproportion in particle size. During the wet season, the surface becomes very slippery and as a result vehicles get stuck and even get veered off the carriageway (Alzubaidi, 1999). Ruts are longitudinal depressions in the wheel tracks resulted by high moisture content in the base, insufficient gravel thickness, and excessive traffic loads (Jones, 1983).

Corrugations are a series of folds and depressions across the gravel surface due to inadequate gravel surface cohesion due to loss of fines (Riverson & Scholer, 1987). Potholes are little dents along the gravel road surface several inches deep resulted by extreme moisture content,

deficient drainage and drainage structures, inadequately graded aggregate, or a mixture of all the listed factors (Frankel & Tahmoorian, 2022). A road with many potholed sections indicates that the road base was poorly done and also that the road may not have been formed to camber or that drainage was not sufficiently provided or that there was excess traffic leading to overloading of the wearing course (Huang, 1961). Depressions are sectional low areas, several millimetres below the adjacent road surfaces produced by settlement, extreme moisture content, and improper drainage (Alzubaidi, 1999). These cover larger areas as compared to potholes. Other indicators of road distress are improper cross sectional area and insufficient drainage.

1.5. Previous studies conducted

In the past, studies have been conducted by various researchers to determine the cause of gravel road deterioration with a few attempts to correlate material properties to the same. In Kenya, Jones (1984) conducted a maintenance study on unpaved roads to investigate deterioration. The main objective of the report was to provide an improved deterioration relationship for unpaved roads for use in a computer model for estimating construction, maintenance and vehicle costs of roads. The research aimed at establishing a relationship between distress features namely gravel lose, surface looseness, roughness, rut depth as well as journey time with traffic loading, climate, geometry, camber and shoulder compaction. Different sections with different gravel compositions were selected for the study. The output was the gravel lose equation later modified to include effect of rainfall in isolation. Overloaded vehicles at the time was found not to have any impact on the roads. The author did not go further into analyzing what properties of the identified gravel namely quartzitic, lateritic, volcanic and sandstone that contributed or rather could be attributed to the distress features identified. This study was able to establish viable models relating the distress features and the material properties of gravel.

In South Africa, Paige-Green (1989) conducted an in-depth study of 'The influence of Geotechnical properties on the performance of gravel wearing course material'. This study aligns to his, and in a section of his study, he correlated distress features with material properties using multiple correlation analysis. He established a single prediction model for each distress parameter. He ascertained their viability through the correlation coefficient. The distresses were dust, stoniness, potholes, cracks, loose material, drainage and erosion, slipperiness, ruts, corrugations and passability. The material properties were similar to those tested in this study. The output was a material specification chart correlating shrinkage product and the grading coefficient. For roads to be all weather Paige noted that adequate material strength was required. This called for a new design procedure that took into account effects of

material quality, traffic, climate, subgrade strength and proper construction procedures as opposed to having a nominal thickness of 150mm. This study came up with this model that captures road deterioration as a factor of material properties for gravel used.

Tadesse (2017) in his work ‘Investigating the effect of wearing course material performance on the serviceability of unpaved gravel roads’ correlated the serviceability rating to the performance of wearing course material, roughness and distress features.

From the correlation between the present serviceability rating and the roughness index, the study established an R^2 correlation of 0.8. The second set of correlation was conducted between material properties namely the grading coefficient (GC), shrinkage product (SP), plasticity index, (PI), liquid (LL) and plastic (PL) limits and the serviceability. The multi linear regression correlation yielded a viable correlation of 0.73. The last correlation is between serviceability and the distress features namely ruts, corrugations, potholes and raveling through multi linear regression. The model yielded a correlation of 0.5 (Tadesse, 2017). This study correlated other material properties, namely; OMC, MDD and CBR which were not captured by Tadesse (2017).

1.6. Research Design and Procedures

The study was conducted using the procedure illustrated in Figure 1.

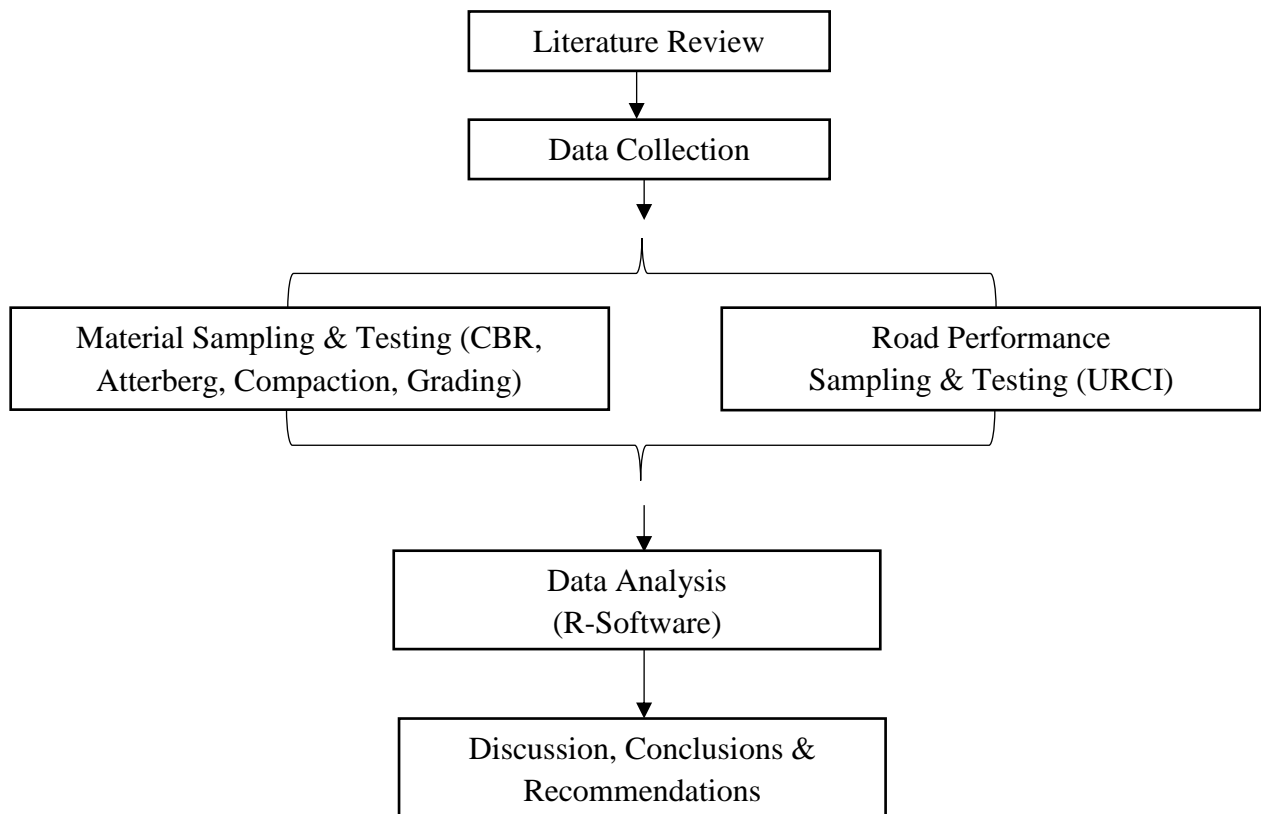


Figure 1: Research Design and Procedures

2. Materials and Methods

2.1. Overview of Methods

Maintenance frequency of gravel roads largely depend on the original construction standard, the traffic load and the prevailing climate. Based on the road condition, repairs are done and in severe cases, reconstruction is done. The quality of material used affects durability of gravel road constructed (Frankel & Tahmoorian, 2022). The correlation between distress features identified on sampled roads and the corresponding laboratory results was determined using simple linear regression. From the regression, the coefficient of correlation R^2 and p -value was obtained.

Bomet County has five sub counties. One road and one borrowpit from each subcounty was sampled. Data collection was done and material testing conducted from five borrow pits located in map as shown in Figure 2. Five roads maintained all in the same year and using gravel from the sampled borrow pits were sampled for assessment. The Unpaved Road Condition Index (URCI) evaluation was conducted on the sampled roads to identify the distress features and their severity. R statistics analysis software was used to correlate the two sets of data obtained. R is the programming language used by the software.

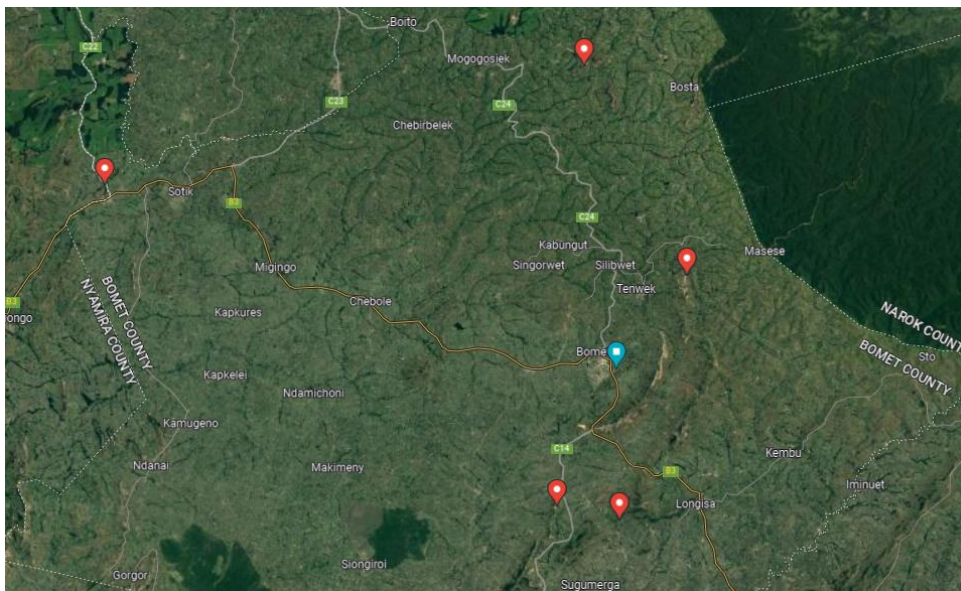


Figure 2: Map of Sampled Borrow Pits (Source: (Google Maps, 2023))

The quality of gravel used for maintenance was tested, three gravel samples were collected at each borrow pit and transported on the same day for testing. Material testing was conducted in accordance with the BS 1377: 1990 specifications. The tests conducted were Particle size distribution/Grading to 0.075mm sieve (BS1377: Part 2: 1990), Atterberg limits (BS1377: Part 2: 1990), Standard Compaction test (BS1377: Part 4: 1990) and CBR (BS1377: Part 4:

1990) and swell at four days soak, on specimens moulded at OMC at three levels of compaction, around 90%, 95% and 100% MDD (Ministry of Works Tanzania, 2000).

Pavement evaluation entails several aspects including structural integrity, structural capacity, roughness and rate of deterioration. Observation of distress features appearing on the surface can be conducted as a form of assessment of the aforementioned factors (Eaton & Beaucham, 1992). The URCI is a numerical indicator based on a scale of 0 to 100. The URCI indicates the road's integrity and surface operational condition. The distresses captured in the survey with respect to extent and severity, across the effective road width were; improper cross section, drainage, corrugations, dust, potholes, ruts, gravel loss and usable width.

The road was first split into sections with the criterion being similarity in characteristics; especially for long roads. The road sections had similar characteristics like traffic, road surface condition, structural composition and construction history. For condition inspection the section was further sub divided into sample units of areas between 140 and 325 square metres. A sample unit measured 30m long, however in cases where the road was under 4.5m width, the length was increased, and reduced for sections with road width greater than 10.5m (Eaton & Beaucham, 1992). Of importance was to select sample sections that were typical of the whole section. Two sample units were required per kilometre and for roads under point eight of a kilometre, one sample unit was taken. For each sample unit the distress parameters were weighted and rated. The URCI was calculated using the following steps; first the distress measurements were recorded in the URCI Sheet individually, second, the density of each distress type was calculated as follows in Equation 3.1 (No density calculation needed for dust).

$$Density = \frac{Amount\ of\ Distress}{Area\ of\ Sample\ Unit} * 100 \dots\dots\dots (1)$$

Using severity level and density, the deduct values were determined from deduct-value curves for each distress type. These were summed up to obtain the Total deduct-value (TDV). The *q* value is the number of individual deduct values greater than five. Using the TDV and *q* from the URCI curve, the URCI for each sample unit was obtained. The road rating was the average of the ratings from all the sample units.

2.2. Analysis of Data Obtained From Materials Testing and URCI

Once data was obtained from the five sampled borrow-pits and roads, the data was analysed to establish a correlation of the two sets of data using R software (Chambers, 2023). R is a language and environment for statistical computing and graphics. The study investigated whether the distress features identified in the road section could be accounted for by the

material properties of the gravel. From the software, the output was the y-intercept, the slope, the *p-value* and correlation coefficient R^2 . For this study the main interest was in the *p-value* and correlation coefficient R^2 .

2.3. Conceptual Framework

The layout of the relationship of the moderating, dependent and independent variables are illustrated in Figure 3.

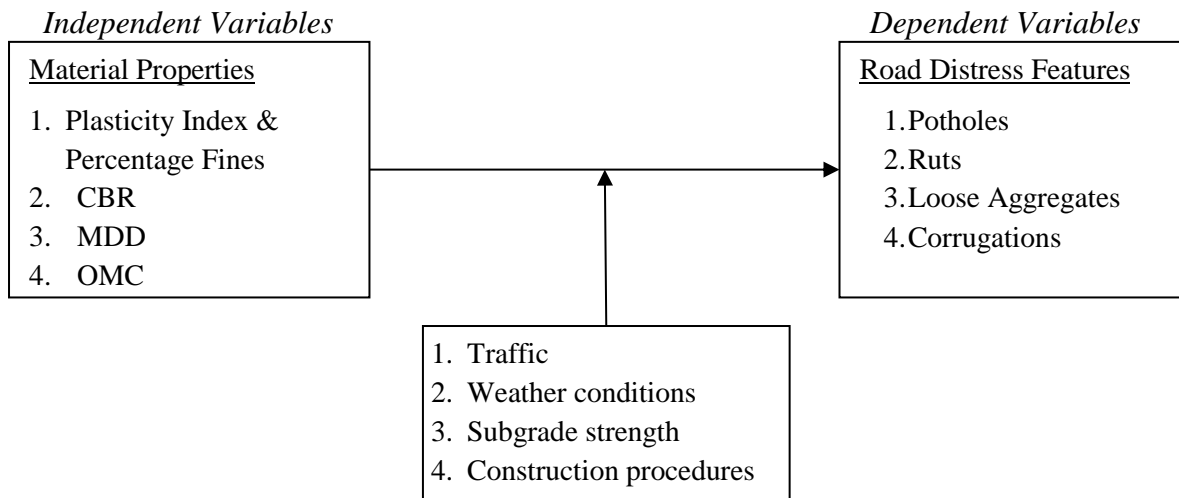


Figure 3: Conceptual Framework of Dependent and Independent Variables

3. Results

3.1. Particle Size Distribution and Atterberg Limits

Gravel consists of a mix of coarse grained particles and fine grained particles. Coarse particles are responsible for strength, high load-bearing capabilities and high drainage abilities. Fines improve binding properties, densification and imperviousness of the road structure. Atterberg limits describe the state of material depending on the moisture content. The particles can either be in solid state, semi-solid state, plastic state or liquid state depending on water content. The results are tabulated in Table 1.

Table 1: Particle Size Distribution and Atterberg Limits results

Borrow pit Sub-County	Sample No.	Grading % Passing BS Sieve Size (mm)						Atterberg Limits				
		20	10	5	2	0.425	0.075	LL	PL	PI	LS	PM
	Required %	95-100	65-100	45-85	30-68	18-44	12-32					
Bomet East	TP1	100	78	59	47	22	17	NON-PLASTIC				
	TP2	100	80	62	49	23	16	38	23	38	23	38
	TP3	100	80	61	45	23	16	39	25	39	25	39
Chepalungu	TP1	100	88	77	59	24	18	31	17	14	7	336
	TP2	100	74	51	28	24	21	53	27	26	14	624

Borrow pit Sub-County	Sample No.	Grading % Passing BS Sieve Size (mm)						Atterberg Limits				
		20	10	5	2	0.425	0.075	LL	PL	PI	LS	PM
		Required %	95-100	65-100	45-85	30-68	18-44					
	TP3	100	85	70	44	20	16	46	23	23	12	460
Bomet Central	TP1	100	85	79	58	21	9	NON-PLASTIC				
	TP2	100	78	64	46	21	14	37	20	17	9	357
	TP3	100	89	68	37	14	7	NON-PLASTIC				
	TP1	100	68	51	40	28	21	54	25	29	15	812
Sotik	TP2	100	56	42	36	39	19	52	29	22	11	858
	TP3	100	76	61	51	39	32	52	31	21	11	819
	TP1	100	76	64	45	14	7	NON-PLASTIC				
Konoin	TP2	100	84	64	39	11	6	NON-PLASTIC				
	TP3	100	78	64	49	18	21	NON-PLASTIC				

3.2. Compaction Test, CBR & Swell

The maximum dry density and optimum moisture content values for every sampled borrow-pit were attained from moisture-density curves plotted from Proctor tests and CBR conducted and displayed in Table 2. CBR measures the ability of material to sufficiently bear loads.

Table 2: Compaction Test Results

Borrow pit Sub-County	Sample No.	Compaction T180			CBR			Swell (%)	Average CBR 95%
		MDD Kg/m ³	OMC (%)	90%	95%	100%			
Bomet East	TP1	2139	9.1	27	61	102	<0.1	59	
	TP2	2146	8.6	29	60	104	<0.1		
	TP3	2151	8.4	25	55	97	<0.1		
Chepalungu	TP1	2155	8.4	15	35	63	<0.1	37	
	TP2	2080	12.2	18	46	81	<0.1		
	TP3	2103	10.4	11	31	48	<0.1		
Bomet Central	TP1	2120	8.3	14	48	75	<0.1	45	
	TP2	1780	14.1	12	45	78	<0.1		
	TP3	2121	8.4	11	43	75	<0.1		
Sotik	TP1	1768	15	10	23	42	<0.1	25	
	TP2	1780	14.1	12	27	43	<0.1		
	TP3	1774	16.3	10	24	40	<0.1		
Konoin	TP1	2020	6	-	-	-	<0.1	0	
	TP2	2044	7.2	-	-	-	<0.1		
	TP3	2050	7.9	-	-	-	<0.1		

3.3.Unpaved Road Condition Index Data

Five roads were sampled, one road per sub-county. The five roads selected were maintained in the same financial year by different implementation teams and contractors. The material used in each road was obtained from different borrow pits, all which were sampled and tested by this study. These roads were proposed for sampling by the respective implementation teams. The equipment used were; a hand odometer, a straight edge, a tape measure and a ruler. The study conducted a windscreen survey driving from start to end of the road, and back while selecting sections to be sampled and marking them. The respective sub-county URCI results were detailed in Table 3.

Table 3: URCI results

Sub County	Section	Sample	Width	Length	Area	Chainage	URCI	Rating	
Bomet East	1	1	4.3	3.7	150.5	0+300	69	48.7	Fair
		2	4.1		164	0+800	45		
	2	3	4.5		148.5	1+000	30		
		4	3.5		150.5	1+800	39		
	3	5	4		148	2+300	37.5		
		6	3.8		129.2	2+600	32.5		
	4	7	3.8		144.4	3+700	88		
Chepalungu	1	1	4.2	3	184.8	0+500	62.5	61.2	Good
		2	4.5		180	1+000	59		
	2	3	4.1		164	1+700	65		
		4	4.4		154	2+000	60		
	3	5	4.2		268.8	2+300	53		
		6	4.7		164.5	2+800	67.5		
Bomet Central	1	1	4.5	3.2	144	0+000	40	66.9	Good
		2	3.3		165	0+700	84		
	2	3	4.1		139.4	1+400	53		
		4	3.3		151.8	1+800	70		
	3	5	3.9		156	2+300	98		
		6	3.7		155.4	2+700	88		
	4	7	3.4		146.2	3+100	35		
Sotik	1	1	4.6	3.4	151.8	0+000	72	71.4	Very Good
		2	4.8		158.4	0+600	60		
	2	3	4		172	1+300	70		
		4	3.9		156	1+800	71		
	3	5	3.9		179.4	2+200	69		
		6	4.5		135	2+900	100		
	4	7	4.6		179.4	3+400	57.5		
Konoin	1	1	4.5	3.3	148.5	0+000	71	61.3	Good
		2	4.5		171	0+600	64		
	2	3	4.8		168	1+200	58		
		4	4.7		164.5	1+800	65		
	3	5	4		160	2+200	45		
		6	4.5		180	2+800	80		
	4	7	4.8		172.8	3+300	46		

3.4. Dependent and Independent Variables

A sample of the data collected from the URCI from Chepalungu is shown in Table 4. The values used for analysis were obtained as a total of the deduct values for each distress feature as a percentage of the total deduct value of all the distress features.

Table 4: Detailed URCI Results

SUB COUNTY	CHEPALUNGU				LENGTH				3KM			
	SECTION	1	SAMPLE	1	SECTION	1	SAMPLE	2	SECTION	2	SAMPLE	3
	LENGTH	44	WIDTH	4.2	LENGTH	40	WIDTH	4.5	LENGTH	40	WIDTH	4.1
	AREA	184.8	CHA	0+500	AREA	180	CHA	1+000	AREA	164	CHA	1+700
DISTRESS	QUANTITY	DENSITY	DV		QUANTITY	DENSITY	DV		QUANTITY	DENSITY	DV	
Improper Cross Section	44.0	23.8	15.0		40.0	22.2	15.0		40.0	24.4	15.0	
Inadequate Roadside Drainage	88.0	47.6	19.0		80.0	44.4	26.0		80.0	48.8	19.0	
Corrugations		0.0			22.4	12.4	8.0			0.0		
Dust		0.0				0.0				0.0		
Potholes		0.0			4.0	2.2	8.0		6.0	3.7	10.0	
Ruts	70.4	38.1	25.0		64.0	35.6	24.0		40.0	24.4	21.0	
		0.0				0.0				0.0		
Loose Aggregate		0.0				0.0				0.0		
	F.Q		TDV	59	F.Q		TDV	81	F.Q		TDV	65
	URCI	62.5	RATING	GOOD	URCI	59	RATING	GOOD	URCI	65	RATING	GOOD

	URCI		61.2				RATING		GOOD				TOTAL INDIVIDUAL DISTRESS DV	TOTAL INDIVIDUAL / TDV	%
	SECTION	2	SAMPLE	4	SECTION	3	SAMPLE	5	SECTION	3	SAMPLE	6			
	LENGTH	35	WIDTH	4.4	LENGTH	64	WIDTH	4.2	LENGTH	35	WIDTH	4.7			
	AREA	154	CHA	2+000	AREA	268.8	CHA	2+300	AREA	164.5	CHA	2+800			
DISTRESS	QUANTITY	DENSITY	DV		QUANTITY	DENSITY	DV		QUANTITY	DENSITY	DV				
Improper Cross Section	35.0	22.7	15.0		64.0	23.8	16.0		35.0	21.3	14.0		90.0	0.214	21
Inadequate Roadside Drainage	70.0	45.5	18.0		64.0	23.8	10.0		70.0	42.6	17.0		109.0	0.260	26
Corrugations		0.0				0.0				0.0			8.0	0.019	2
Dust		0.0				0.0				0.0			0.0	0	0
Potholes		0.0				0.0				0.0			18.0	0.042	4
Ruts	24.0	15.6	17.0		89.6	33.3	23.5		44.5	27.1	22.5		133.0	0.317	32
		0.0			89.6	33.3	30.0			0.0			30.0	0.071	7
Loose Aggregate	105.0	68.2	20.0		66.6	24.8	11.0			0.0			31.0	0.073	7
	F.Q		TDV	70	F.Q		TDV	90.5	F.Q		TDV	53.5	419.0		
	URCI	60	RATING	GOOD	URCI	53	RATING	FAIR	URCI	67.5	RATING	GOOD			

The dependent variables for all the sub-counties are tabulated in Table 5;

Table 5: Dependent Variables

Sub-County Distress Features	Konoin	Sotik	Bomet Central	Bomet East	Chepalungu
Improper Cross Section	20	16	31	22	21
Inadequate Roadside Drainage	29	48	19	20	26
Corrugations	0	13	0	4	2
Dust	0	2	0	0	0
Potholes	1	6	4	5	4
Ruts	14	6	27	36	39
Loose Aggregate	36	9	18	13	7
URCI	61.3	71.4	66.9	48.7	61.2

Of the seven parameters the study selected corrugations, potholes, ruts and loose aggregates to be used for analysis based on the frequency of occurrence.

The independent variables used are tabulated in Table 6;

Table 6: Independent Variables

Sub-County Material Properties	Konoin	Sotik	Bomet Central	Bomet East	Chepalungu
% Fines (Passing Sieve 0.075)	11	24	10	16	18
PI	1	24	17	15	21
MDD (Kg/m ³)	2038	1774	2007	2145	2113
OMC (95%)	7	15	10	9	10
CBR	1	25	45	59	37

3.5. Regression Analysis

To examine the correlation of the distress to the material properties, regression analysis was used. The dependent variables were the distress parameters namely loose aggregates, corrugations, ruts and potholes; and the independent variables were the material properties.

The independent variables were analysed against each dependent variable through simple linear regression to establish whether a direct linear relationship exists. The analyses were done through R Studio Software. Significance of the correlation was ascertained by assessing the p -value and R^2 value. The p -value evaluates the probability that the results attained in the model occurred by chance. A p -value of less than 0.05 was statistically required for a model to be considered significant; on the basis of a 95% percent confidence interval; which implies that the results of the model would occur by chance alone only five times in every 100 trials (Hesham, Christina, & Ali, 2011). The R^2 value shows the percentage of the total variance in the dependent variable explained by the independent variable; therefore, a value close to 1.000 is ideal. The values of the models generated were tabulated in Table 7.

Table 7: Correlation Coefficients and P-Values

	<i>Loose Aggregates</i>		<i>Corrugations</i>		<i>Ruts</i>		<i>Potholes</i>	
	<i>R²</i>	<i>P</i>	<i>R²</i>	<i>P</i>	<i>R²</i>	<i>P</i>	<i>R²</i>	<i>P</i>
Percentage fines	0.4931	0.1861	0.8309	0.0312	0.0645	0.6801	0.5329	0.1614
Plasticity Index	0.9137	0.0111	0.3757	0.1861	0.0209	0.8162	0.8158	0.0356
OMC	0.4553	0.2116	0.805	0.0389	0.188	0.4658	0.665	0.0925
MDD	0.0169	0.8347	0.588	0.1303	0.7435	0.0601	0.1495	0.5202
CBR	0.3935	0.2573	0.0011	0.9574	0.5123	0.174	0.3764	0.2711

Some parameters were strongly correlated and yielded significant models while others barely had any correlation. The simple linear regression produced several significant models. From the loose aggregate simple linear regression, the plasticity index variable yielded a significant model with a *p-value* of 0.01 and an R^2 value of 0.91 Figure 4(a) below. For corrugations, the independent variables were percentage fines with *p* value of 0.03118 Figure 4 (b) and Optimum Moisture content with a *p-value* of 0.03896 in Figure 5(a) and an R^2 value of 0.8 for both. The simple linear regression for ruts also yielded a significant model for the independent variable maximum dry density with a *p-value* of 0.06 and an R^2 value of 0.74 Figure 5(b).

Potholes also correlated with plasticity index with a *p-value* of 0.036 and correlation coefficient R^2 of 0.82 and significantly as well with OMC with a *p-value* of 0.09 and R^2 value of 0.7 as shown in Figure 6 (a) and (b). This means that for all the significant models above, the variance and degree of distress can be associated with the respective variables.

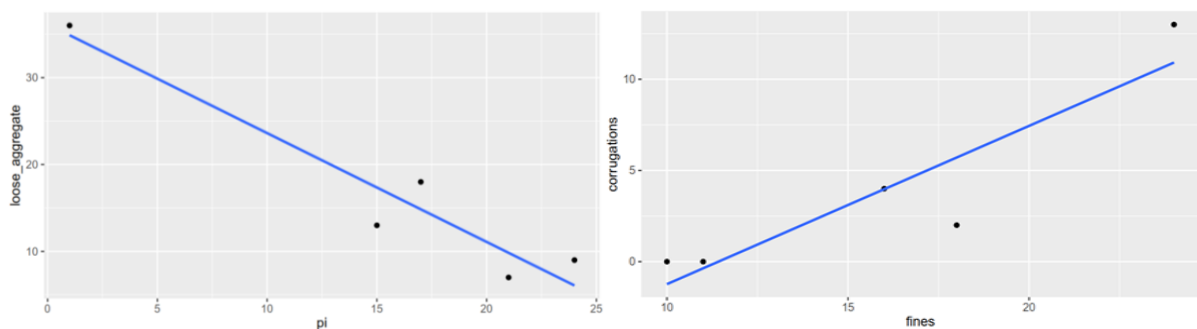


Figure 4: (a) PI vs. Loose aggregates plot (b) Percentage fines vs. Corrugations plot

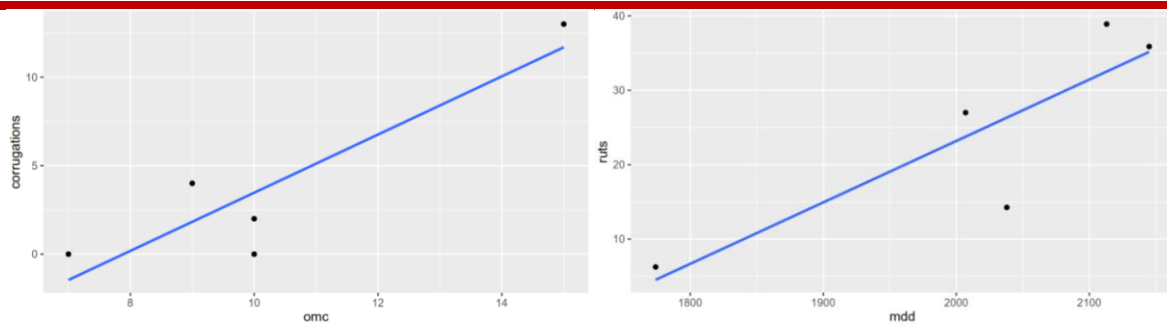


Figure 5: (a) OMC vs. Corrugations plot (b) MDD vs. Rutting plot

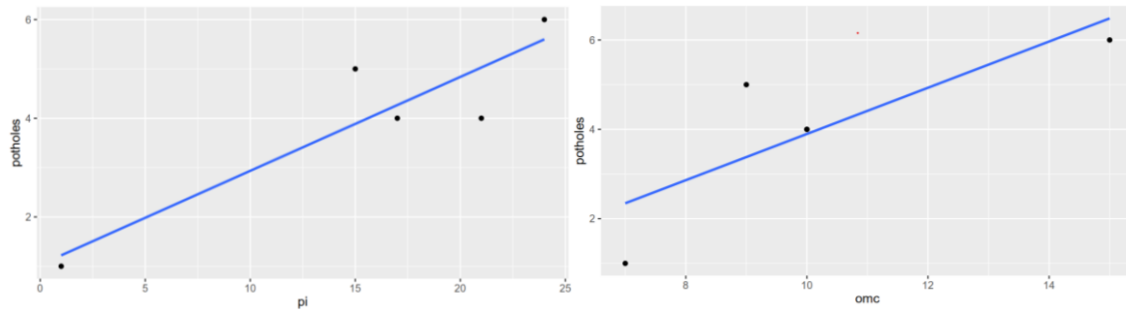


Figure 6: (a) PI vs. Potholes plot (b) OMC vs. Potholes plot

4. Discussion of Results

4.1. Correlation between Plasticity Index and Loose Aggregates

From the loose aggregates simple linear regression, the plasticity index variable produced a significant model having a p-value of 0.01 and an R^2 value of 0.91. The two variables have a negative correlation meaning the higher the plasticity index, the lower the amount of loose aggregates present.

$$y = -0.7384x + 27.889 \dots \dots \dots (2)$$

Plasticity Index is a factor of fines, the two are directly proportional. The presence of sufficient amount of fines in gravel is important in terms of binding the structure together. Cohesion varies with moisture and amount of fines. When both moisture and fines are in excess, gravel loses the adhesive effect due to expansion of the solids framework, causing a loss in mechanical contact through excessive volume change. As a result vehicles lack adequate grip get stuck along the carriageway, in this case the fines acts as a lubricant more than a binding element (Paige-Green, 1989). However, with minimum moisture conditions, fines do not develop the cohesion needed to resist surface abrasion, which leads to loss of gravel and dust. Loose aggregates on a road surface are a result of insufficient adhesion between fine and coarse particles in the gravel surface material. Loss of fine particles further results in presence of rough patches on the surface (Adlinge & Gupta, 2018).

4.2. Correlation between Percentage Fines and Corrugations

From the corrugations simple linear regression, the percentage fines variable yielded a meaningful model having a *p-value* of 0.01 and an R^2 value of 0.91.

$$y = 0.9658x + 12.174 \quad (3)$$

The correlation was positive, meaning an increase in fines beyond a certain point results in an increase in corrugations. 99% of corrugations occurrence were in conjunction with the amount of percentage fines and plasticity index of the gravel. Fines act as a binder and improve cohesion of particles and resistance to abrasion. However when in excess and in different weather seasons, the cohesion is affected. In rainy season, the fines absorb the moisture and therefore swells leading to slipperiness and displacement of coarse particles under traffic loading.

4.3. Correlation between Optimum Moisture Content and Corrugations

From the corrugations simple linear regression, the OMC variable generated a significant model with a *p-value* of 0.03 and an R^2 value of 0.8.

$$y = 0.4941x + 8.3452 \quad (4)$$

The positive correlation implies an increase in moisture content beyond the OMC results in increase in occurrence of corrugations. 97% of corrugations developed are related to OMC

Moisture content is varied accordingly during compaction of gravel roads. Compaction decreases wearing course permeability and improves water shedding capacities. When water is too little, compaction is not evenly done to enable the road structure to attain its maximum density and strength. When the water is in excess, the fines in the gravel absorb the moisture hence reducing the density and resistance to deformation. When moisture is in excess the particles also lose the cohesiveness and get viscous. The water fills the voids almost completely keeping the soil particles apart hence leading to a drop in density. Upon further traffic loading, the weakened section ravel further and forms corrugations.

4.4. Correlation between Maximum Dry Density and Rutting

There exists a positive correlation between MDD and rutting. The simple linear regression produced a viable output with a *p-value* of 0.06 and an R^2 value of 0.07.

$$y = 9.0039x + 1795.2 \quad (5)$$

. A gradual increase in the MDD results in an increase in the probability of rut formation. 94% of ruts occurring are as a result of MDD. Ruts are caused by a permanent deformation in any of

the road layers or subgrade. They result from repeated vehicle passes, especially when the road is soft and not well compacted to MDD. When a heavily compacted soil mass undergoes shear loading, it has a tendency to expand. This expansion that occurs is uneven, hence some areas are weaker than other parts. This loosening enables water to permeate more easily hence weakening the road structure. Soils that are heavily compacted beyond the MDD display sudden decline in strength under shear loads, leading to displacement of particles leading to rut formation. When compacted, the material becomes self stabilised and properly stiffened hence spreading traffic loads better. This improved load spreading reduces stresses to the subgrade hence reducing the amount and risk of rutting (Dawson, Kolisoja, Vuorimies, & Saarenketo, 2007).

4.5. Correlation between Plasticity Index and Potholes

From the potholes simple linear regression, the plasticity index variable generated a significant model with a *p-value* of 0.03 and an R^2 value of 0.81.

$$y = 4.5365x - 3.1465 \quad (6)$$

The correlation is positive, meaning an increase in Plasticity Index beyond a certain point results in increase in pothole development. 97% of potholes occurrence are in conjunction to amount of fines and plasticity index of the gravel. Potholes are produced when traffic wears away fines of the road surface. They grow faster when water collects inside the indent created. The road continues to disintegrate because of loosening surface material and formation of weak spots in the underlying soils. Plasticity index is a factor of fines especially clays. Fines have a binding effect on road surface particles. The fines bind together the coarse aggregate enabling it to resist abrasion. A high amount of fines also affects the strength of the structure as a result of increased swelling and shrinkage. This leads to weak areas in the compacted structure which allows water to penetrate. Upon continuous loading and wet conditions this further leads to ponding and displacement of particles leading to road failure. Therefore, sufficient grading is required to ensure that the amount of fines is in adequate quantities (Paige-Green, 1989).

4.6. Correlation between Optimum Moisture Content and potholes

From the potholes simple linear regression, the OMC variable yielded a viable model with a *p-value* of 0.09 and an R^2 value of 0.7.

$$y = 1.3521x + 4.6126 \quad (7)$$

The positive correlation is denotes an increase in moisture content beyond OMC results in increase in pothole formation. 91% of potholes occurrence were due to moisture related conditions. Excess moisture together with traffic action weaken the pavement by reducing its bearing strength. Moisture content at optimum enables better compaction of the gravel particles by replacing the air particles and binding the gravel fines and coarse aggregates. Beyond OMC, the adhesion and cohesion of the moisture decreases and instead results in displacement of particles. This decrease results in weaker bonds between the fines and the coarse aggregates, these bonds cannot withstand vehicular loading. This therefore results in displacement of particles. Constant displacements leads to forming of depressions which trap more moisture and the cycle repeats itself upon loading leading to pothole formation. Pothole formation is also a factor of inadequate drainage and poor road formation. A gravel surface that is well formed with a proper crown and sloped shoulders facilitates quick removal of water from the surface. When the water is retained for long periods on the road surface, the material softens and under traffic loading develops small pits. These small pits hold wter which further softens the compacted surface and the suspended fine particles are displaced by traffic. The coaser particles no longer held by a binder is also displaced during dry conditions, eventually developing into large potholes.

5. Conclusions and Recommendations

5.1. Conclusions

The conclusions from the research were; a significant model was established indicating a direct negative correlation of 0.9 between the gravel plasticity and the amount of loose aggregates present. A positive correlation of 0.8 and 0.8 between percentage fines, moisture content and corrugations was established. A significant model was established indicating a positive correlation of 0.7 between MDD and rutting. A positive correlation of 0.8 and 0.7 between plasticity index, OMC and potholes was determined. Therefore, the study concluded that the findings were evidence that indeed quality gravel is important for sustainable and durable infrastructure. Incorporation of the findings in the design and implementation of gravel roads allows for mitigation of future distress features before occurrence.

It was almost impossible to study independently the effect on material properties on road distresses and performance. Factors like traffic, road formation, rain, terrain, road formation & compaction, gravel layer thickness and drainage provision all play a role in the deterioration of roads. The above features also affect the material properties in one way or another. Good construction procedures are mandatory, moisture compaction alone improves the strength and

bearing capacity of the gravel greatly. This research however attempted to isolate the material geotechnical properties and their effect in road deterioration; since they are key parameters.

5.2.Recommendations

Ideally, gravel roads require maintenance as soon as distress features begin to appear. When the distresses are not repaired, the road completely fails, leading to reconstruction, which is much more costly. Selecting the appropriate gravel material is essential for construction of durable infrastructure. Therefore, mandatory sampling and testing of the existing subgrade soil along the carriageway as well as materials from borrow pits to be selected, should be enforced in the design stage. The study confirmed the correlation of appearance of distress features on roads to material properties. In the event that gravel does not meet the required standard, blending is recommended in some instances, while in other instances, the sample is rejected requiring an alternative. Workmanship affects road performance and during compaction, moisture should be closely monitored to ensure that OMC is attained for optimum compaction.

5.3.Recommendations for further study

1. A larger sample area and longer study duration could be utilized for further research.
2. The correlation between CBR and distress features loose aggregates, corrugations, ruts and potholes should be further investigated.
3. Include traffic, subgrade material and meteorological factors to the variables to establish correlation with road performance.
4. Further investigation of effect of percentage fines, MDD and OMC on potholes.
5. A multi linear regression could be done to come up with a road deterioration model with regards to material properties
6. Other quantitative methods of assessing road condition could be utilised.

References

- Federal Highways Authority. (2015). *Gravel Roads construction & maintenance guide*. South Dakota: South Dakota State University.
- Jones , T. E., Robinson , R., & Snaith, M. S. (1984). A field study on the deterioration of unpaved roads and the effect of different maintenance strategies. *Regional Conference for Africa on Soil Mechnaics and Foundation Engineering* (p. 13). Harare: TRRL Laboratory report 673.
- Adlinge, S. S., & Gupta, A. K. (2018). Pavement Deterioration and its Causes. *IOSR Journal of Mechanical & Civil Engineering (IOSR-JMCE)*, 7.
- Alzubaidi, H. (1999). *Operation and Maintenance of Gravel roads*. Linkoping: Swedish National Roads Administraton.
- Alzubaidi, H., & Magnusson, R. (2002). Deterioration and Rating of Gravel Roads. *Road Materials and Pavement Design*, 27.
- Andrew R. Dawson, P. K. (2007). Design of Low-Volume Pavements Against Rutting. *Transportation Research Record 1989*, 8.
- Chambers, J. (2023, June 16). R Software. (R version 4.3.1 (Beagle Scouts)). -, -, -. Retrieved from <https://www.r-project.org/>
- Da Silva, M. F., Ribeiro, M. P., Furlan, A. P., & Fabbri, G. P. (2021). Effect of compaction water content and stress ratio on permanent deformation of a subgrade lateritic soil. *Transportation Geotechnics, Volume 26*, 9.
- Dawson, A. R., Kolisoja, P., Vuorimies, N., & Saarenketo, T. (2007). Design of Low-Volume Pavements Against Rutting. *Transportation Research Record 1989*, 8.
- Eaton, R. A., & Beaucham, R. E. (1992). *Unsurfaced Road Maintenance Management*. Virginia: United States Army Technical Manual.
- Frankel, J., & Tahmoorian, F. (2022). Improving Gravel Material Specifications for Unpaved Roads:. *International Journal of Pavement Research and Technology*, 14.
- Google Maps. (2023, April 3). *Google Maps*. Retrieved from Google Maps: <https://maps.app.goo.gl/NKXfctsbkP9o2BsbA>

- Hesham M, C. B. (2011). Analysis of Factors Causing Corrugation of Gravel Roads. *Transportation Research Record 2204*, 8.
- Hesham, M., Christina, B., & Ali, S. (2011). Analysis of Factors Causing Corrugation of Gravel Roads. *Transportation Research Record 2204*, 8.
- Huang, E. Y. (1961). A study of occurrence of Potholes and washboards and soil aggregate roads. *39th Annual Meeting of the Highway Research Board* (p. 25). Washington DC: Highway Research Board.
- Jones, T. E. (1983). The Kenya maintenance study on unpaved roads: Research on deterioration. *Transport and Road Research Laboratory*, 54.
- Jones, T. E. (1984). *The Kenya Maintenance study on unpaved roads: Research on Deterioration*. Transport and Road Research Laboratory, Department of Transport. Crowthorne: Transport and Road Research Laboratory.
- Matheus Francisco da Silva, M. M. (2021). Effect of compaction water content and stress ratio on permanent deformation of a subgrade lateritic soil. *Transportation Geotechnics, Volume 26*, 9.
- Ministry of Transport. (1987). *Road Design Manual*. Nairobi: Ministry of Transport.
- Ministry of Works Tanzania. (2000). *Laboratory Testing Manual*. Daresalaam: Novum Grafisk AS.
- Paige-Green, P. (1989). *The influence of Geotechnical properties on the performance of gravel wearing course material*. Pretoria: University of Pretoria.
- Riverson, J. D., & Scholer, C. F. (1987). *A Road Maintenance Management Information System for Counties and Cities*. Indiana.
- Sharad.S.Adlinge, P. (2018). Pavement Deterioration and its Causes . *IOSR Journal of Mechanical & Civil Engineering (IOSR-JMCE)*, 7.
- Skorseth, K. (2000). *Gravel Roads Maintenance and design manual*. South Dakota: Federal Highway Administration.
- Sunley, W. T. (1996, May 1). Water- Road's number one enemy. *Illinois Municipal Review*, p. 1.

Tadesse, H. F. (2017). *Investigating the effect of wearing course material performance on the serviceability of unpaved gravel roads*. Hawassa: Hawassa University.

Transport & ICT. (2016). *Measuring Rural Access: Using New Technologies*. Washington DC: World Bank.

Yellow Rivers Watershed Management Authority. (2000). *Guideline For Maintenance And Service Of Unpaved Roads*. China: Yellow Rivers Watershed Management Authority.

Evaluation of the Effectiveness of Rice Straw Fibres on Expanded Polystyrene Lightweight Concrete

W. O. Mocha*, S. W. Mumenya, S. O Abuodha

Department of Civil and Construction Engineering, University of Nairobi, Kenya.

*Corresponding author: mochawislay@gmail.com

Article History

Submission Date: 8th October 2024

Acceptance Date: 15th November 2024

Publication Date: 31st December 2024

Abstract

The increasing necessity of sustainable construction materials has led the research for new alternatives that diminish environmental damage and the depletion of natural resources. In this study, Rice Straw Fibres (RSF) and Expanded Polystyrene aggregates were investigated to produce an environmentally friendly lightweight concrete composite. Like other lightweight materials, EPS can cause a reduction in concrete weight but also tensile and flexure strength capabilities. In this research, RSF as renewable natural fibre reinforced within the composite to reduce those drawbacks and simultaneously improve mechanical properties of the composite. The aims of this research were studying the physical and mechanical properties associated with RSF and EPS, evaluating performance of new developed composite, identifying an optimum mixing ratio and examining its applicability for structural applications. Concrete mixes with a water-to-cement ratio of 0.6 were prepared, with fine aggregates replaced by 10% EPS beads by volume, and RSF added in varying amounts (0%, 0.5%, 1.0%, and 1.5%). The results revealed that the inclusion of RSF improved tensile and flexural strength, addressing the weaknesses caused by EPS in the composite. Specifically, the mix with 10% EPS and 1.0% RSF offered the best balance of mechanical properties, including crack resistance and weight reduction, while maintaining acceptable compressive strength. The composite demonstrated a marked reduction in density, making it suitable for lightweight construction.

Keywords - Rice Straw Fibres (RSF), Expanded Polystyrene (EPS), lightweight concrete, recyclable material, mechanical properties, sustainability.

1. Introduction

Composites combine independent material constituents to form a material with superior performance properties. They have been used in the construction sector for many years due to its improved performance. Two significant challenges still persist: the demand that plastic waste not to leave a trace in landfills, especially non-biodegradable single use plastics such as polystyrene; and the depletion of resources needed to build them. These factors underline the need for more eco-friendly alternatives. In this study, the investigation is proposed to partially replace conventional fine aggregates with recycled expanded polystyrene (EPS) in concrete and replacing rice straw fibres (RSF) as an additional binder. The aim is to create an environmentally friendly composite useful for both structural and non-structural fields.

Even today, concrete is one of the most popular construction materials, producing over 11 billion metric tons annually (Sheheryar & Nehdi, 2021). However, its drawbacks, such as low tensile strength and susceptibility to shrinkage, are well-known (Mukhdomi et al., 2021). Lightweight concrete (LWC) is widely adopted due to its reduced weight and improved thermal properties. Expanded polystyrene (EPS), a common material in LWC, has been shown to reduce concrete density and weight.

2. Literature Review

Research shows that the size of EPS beads significantly impacts compressive strength, with smaller beads resulting in stronger concrete. However, EPS concrete can suffer from issues like segregation and moisture absorption, particularly with larger beads (Prasittisopin et al., 2022).

Rice straw, a byproduct of rice production, has emerged as a potential reinforcement material in concrete. When treated properly, rice straw fibres can enhance the tensile and flexural strength of concrete composites, making it a promising option for sustainable construction (Lv et al., 2022).

Despite the advantages of using EPS in LWC, challenges remain. EPS concrete often requires more cement and has lower resistance to concentrated loads, sensitivity to water content, longer mixing times, and placement difficulties. Additionally, issues like shrinkage-induced microcracks and increased water absorption have been observed (Aljalawi, 2019). Fibres, particularly natural fibres like RSF, can help overcome these drawbacks by improving impact resistance, tensile and flexural strength, and minimizing dry shrinkage. Fibres also enhance crack resistance, a critical benefit in concrete applications (Ahmad et al., 2022).

This study evaluated the effectiveness of combining recycled EPS and rice straw fibres to improve the physical and mechanical properties of lightweight concrete. The assessments include compressive, tensile, and flexural strengths, workability, and permeability properties, comparing the new composite with conventional concrete to determine its suitability for lightweight structural applications. This research also addresses environmental concerns by finding a practical use for polystyrene waste and rice straw, thus reducing pollution while preserving natural resources in the construction industry.

3. Methodology

3.1. Material Sources and Preparation

The raw materials employed were recycled polystyrene, rice straw fibres, fine aggregates, coarse aggregates, Portland pozzolana cement, and water.

3.1.1. Recycled Expanded Polystyrene (EPS)

Recycled polystyrene was sourced from major dump sites around Nairobi, sorted, and thoroughly cleaned. The EPS, is as shown in Figure 3.1.



Figure 3.1: Discarded Expanded Polystyrene (EPS) used for transporting good and EPS in beads form

3.1.2. Rice straw fibres (RSF)

Rice straw, shown in Figure 3.3, was sourced from the Mwea irrigation scheme. The straw was cleaned, cut into lengths of 150 to 300 mm, and treated with a 1% sodium hydroxide (NaOH) solution for 24 hours to reduce brittleness. This method was based on the recommendations of Derman et al. (2022). After treatment, the straw was washed until the rinsing water was clear, mechanically blended for 5–6 seconds, and dried at 150°C.



Figure 3.3: Rice straw fibres

3.2. Proportions of the various mixes

A control mix (M1) was prepared using a ratio of 3 coarse aggregates to 1.5 fine aggregates to 1 cement. In the remaining mixes, 10% EPS replaced fine aggregates. The proportions of RSF added were 0, 0.5, 1.0, and 1.5% by mix volume. The optimal proportion of RSF was determined based on the mixes summarized in Table 3.1

Table 3.8 Proportions of the various mixes

MIXES	CEMENT	FINE AGGREGATES	COARSE AGGREGATES	EXPANDED POLYSTYRENE (EPS)	RICE STRAW FIBERS (RSF)
M1 (control)	100%	100%	100%	-----	-----
M2	100%	90%	100%	10%	-----
M3	100%	89.5%	100%	10%	0.5%
M4	100%	89.0%	100%	10%	1.0%
M5	100%	88.5%	100%	10%	1.5%

3.3. Laboratory Tests

Fine and Coarse Aggregates: Testing was conducted according to BS EN 12620 and BS EN 933 to establish roundness, angularity, flakiness index, aggregate crushing, moisture content, and particle size distribution.

Rice Straw Fibre (RSF): Properties such as density, diameter, average length, aspect ratio, and tensile strength were evaluated. The fresh concrete: underwent various tests like slump test, degree of compactability, and density tests, following the guidelines provided in the BS EN 12350 series to evaluate its characteristics and performance. Hardened concrete was subjected to compressive, tensile, splitting strength, density, and water absorption tests according to BS EN 12390 series guidelines to assess its properties over 7,14 and 28 days.

4. Results, Analysis and Discussion

4.1. Results

4.1.1 Physical Properties of Raw Materials

The tests conducted on the raw materials were essential to evaluate their characteristics and ensure they meet the requirements for producing high-quality concrete. The physical properties of the raw materials, are summarized in Table 4.1

Table 4.1 Physical Properties of Raw Materials

	Fine Aggregate	Coarse Aggregate	EPS	RSF
Saturated Surface Dried (SSD) (g)	456.1	506.6	6.6	30.7
Pycnometer + Water + SSD (g)	1880.8	1918.8	1507.3	1609.6
Pycnometer + Water (g)	1611.3	1611.3	1611.3	1611.3
Oven Dried (g)	446.1	491.6	3.4	9.0
Water Absorption (%)	2.24	3.06	94.12	241.11
Specific Gravity	2.53	2.54	0.03	0.84
Density (kg/m ³)	1675	1500	19.7	118.14
Rice Starw Fiber (RSF) results				
Density (D)				118.14 kg/m ³
Diameter (D),				4 mm
Average Length (L),				200 mm
Aspect Ratio (L/D),				50
Tensile Strength (T)				4.19 MPa

Sieve analysis results demonstrated that all aggregates exhibit suitable particle size distributions for concrete production. The fine aggregates are well-graded for workability and the coarse aggregates provide strength and stability making them ideal for the intended concrete mix designs.

4.1.2 Results of Fresh Concrete Tests

Slump value, compaction factor and density of the fresh concrete are presented in table 4.5

Table 4.5: Results of Fresh Concrete Tests

Mix	Slump Value (mm)	Remarks (Satisfactory/ Fail)	Compaction Factor	Density (kg/m ³)	Water Absorption (%)
M1 (control)	70	Satisfactory	0.923	2300	2.83
M2	55	Satisfactory	0.923	2260	3.2
M3	47	Satisfactory	0.992	2240	3.58
M4	40	Satisfactory	0.979	2270	3.9
M5	35	Satisfactory	0.983	2220	5.11

The incorporation of Expanded Polystyrene (EPS) and Rice Straw Fibers (RSF) reduces concrete density due to their lightweight and porous nature compared to traditional aggregates. EPS creates a more porous structure, and RSF increases air voids, further lowering mass per unit volume. Higher RSF content leads to greater voids and reduced density. Water absorption also increases with the addition of EPS and RSF, rising from 3.58% (0.5% RSF) to 5.11% (1.5% RSF), as RSF's hydrophilic properties and porosity enhance the concrete's ability to absorb water.

4.1.3 Mechanical Properties of Hardened Concrete

Summary Table of Compressive, Tensile, and Flexural Strength at Different Days for the Conventional concrete, Concrete with EPS, and Concrete with EPS and RSF in varied proportions are presented in tables 4.6, 4.7 and 4.8 respectively. The graphs for compressive strength, tensile strength, flexural strength, and water absorption for the 28-day results of the different mixes are presented in Figures 4.6, 4.7, and 4.8 respectively.

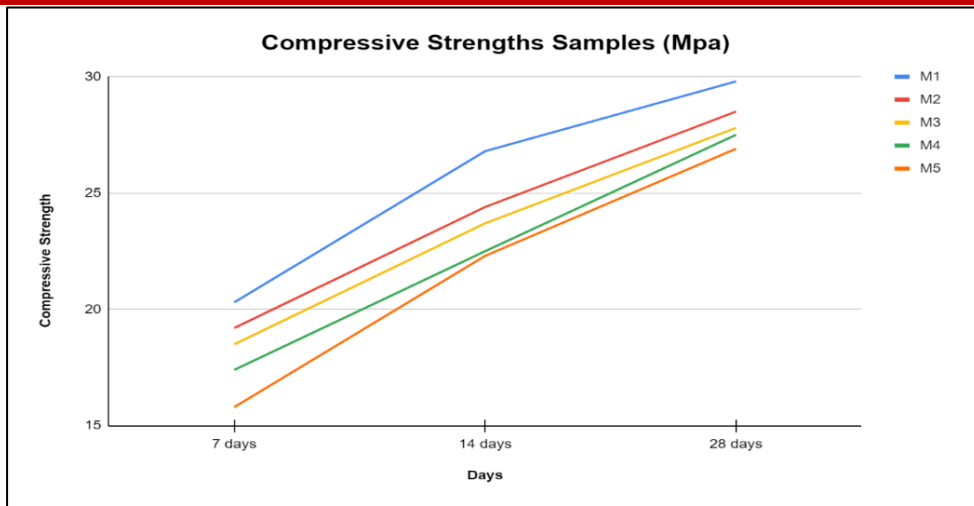


Figure 4.6 Compressive Strength (MPa) of the mixes at 7,14 and 28 days

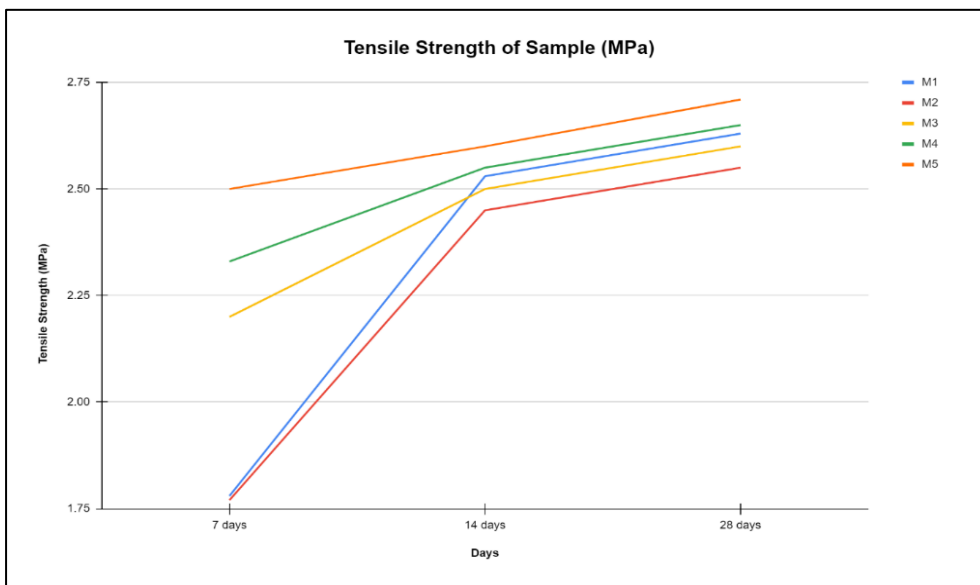


Figure 4.7 Tensile strengths of the mixes at 7, 14 and 28 days

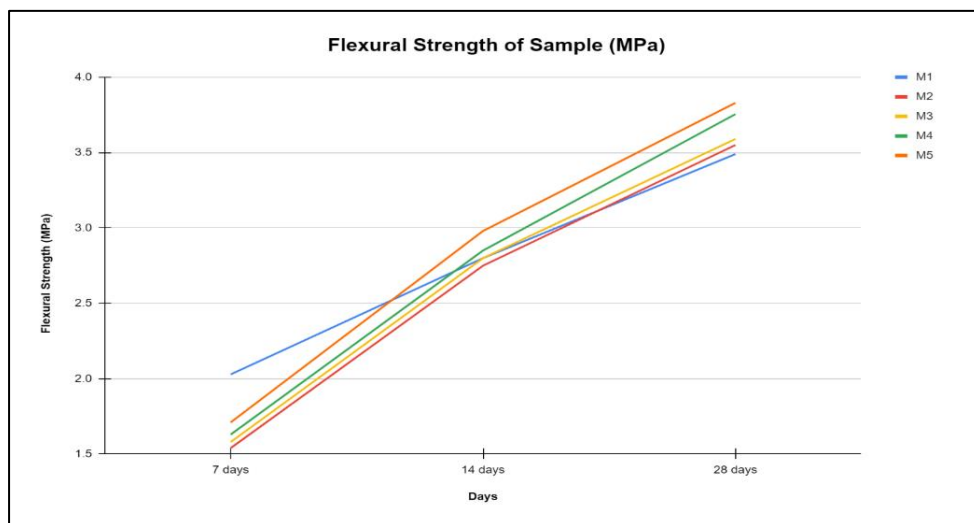


Figure 4.8 Flexural strengths of the mixes at 7, 14 and 28days

Table 4.6: Conventional concrete results

Days	Compressive Strength (MPa)	Tensile Strength (MPa)	Flexural Strength (MPa)	Density (kg/m ³)
7 Days	20.3	1.78	2.03	2252
14 Days	26.8	2.53	2.80	2271
28 Days	29.8	2.63	3.49	2300

Conventional concrete exhibited lower tensile and flexural strengths compared to its compressive strength. Even at 28 days, the tensile and flexural strengths reached only 2.63 MPa and 3.49 MPa, respectively, which is still lower than what might be desired for certain structural applications. This indicates that while Conventional concrete offers high compressive strength, it may not be ideal where significant tensile or bending forces are expected.

Table 4.7: Concrete with EPS added.

Days	Compressive Strength (MPa)	Tensile Strength (MPa)	Flexural Strength (MPa)	Density (kg/m ³)
7 Days	19.2	1.77	1.54	2250
14 Days	24.4	2.45	2.75	2267
28 Days	28.5	2.55	3.55	2260

The inclusion of EPS resulted in lightweight concrete with acceptable strength development over time. The compressive strength at 28 days reached 28.5 MPa, exceeding the target for Class 20/25 concrete. While the tensile and flexural strengths were slightly lower than that of Conventional concrete, the values were sufficient for applications where lightweight concrete is preferred. The mix maintained a steady strength development, proving that the use of EPS effectively reduces the weight of the concrete without significantly compromising its structural integrity. Figure 4.9a and figure 4.9b illustrate samples which have undergone tensile splitting test failure and flexural failure.

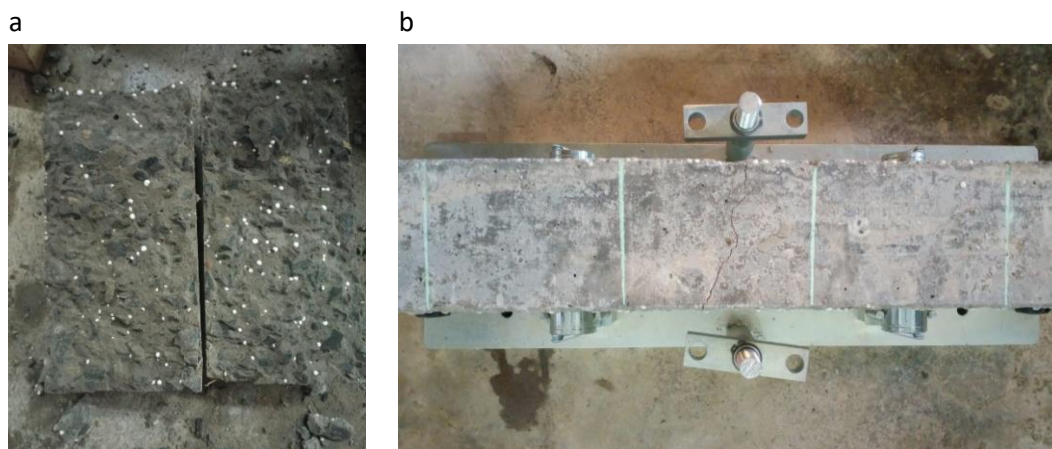


Figure 4.9 Samples which have undergone tests failure

Table 4.8: Concrete with EPS and RSF added

Days	Mix	Compressive Strength (MPa)	Tensile Strength (MPa)	Flexural Strength (MPa)	Density (kg/m ³)
7 Days	M3	19.2	2.20	1.58	2222
	M4	18.1	2.33	1.63	2163
	M5	15.8	1.82	1.71	2193
14 Days	M3	24.2	2.50	2.8	2252
	M4	22.5	2.55	2.85	2222
	M5	22.3	2.30	2.98	2222
28 Days	M3	27.8	2.60	3.59	2240
	M4	27.5	2.65	3.755	2270
	M5	27.7	2.50	3.83	2220

The addition of both EPS and RSF improved the tensile and flexural strengths of the concrete. Mix M3 to M5 exhibited enhanced tensile and flexural performance compared to concrete without RSF. The compressive strengths for these mixes were also acceptable, with values of around 27.5 MPa at 28 days, exceeding the 25 MPa target for Class 20/25 concrete. This indicates that combining EPS with RSF enhances the flexibility and resistance to tensile forces while maintaining the required compressive strength for structural use.

4.2. Discussion

4.2.1 Properties of the Raw Materials

The performance of concrete mixtures is greatly determined by physical and mechanical characteristics of constituents. Water absorption, for example, influences the water-cement ratio and as a result the strength of the mix. The RSF showed a tensile strength of 4.19 MPa, a low density of 118.14 kg/m³, and an aspect ratio of 50. These characteristics propose that RSF should be able to improve ductility and energy absorption of the lightweight concrete by virtue of its incorporation. Using high aspect ratio of RSF also enables effective load distribution throughout the matrix and enables good adhesion of the cement paste.

EPS weighed only 19.7 kg/m in volume and a specific density of 0.03 hence, reducing the overall weight of the concrete mix. As a result, EPS materials are recommendable in places where weight reduction is a major consideration.

Both RSF and EPS can contribute positively to the lightweight concrete matrix, but careful consideration of their properties is essential for achieving the desired mechanical performance. The high-water absorption rates of 241.11% for RSF and 94.12% for EPS may require adjustments in the water-cement ratio and the potential use of superplasticizers to enhance workability without compromising strength. Thereby enhancing the use of sustainable materials in construction.

4.2.2 Performance of the Newly Developed Composite

The newly developed composites exhibited lower densities, resulting in lightweight concrete. This reduction in density can be attributed to the low density and minimal water absorption of EPS. As a result, the EPS-added concrete (M2) demonstrated a slight decrease in compressive strength, reaching 28.5 MPa at 28 days, compared to the compressive strength of conventional concrete (M1), which exhibited 29.8 MPa at the same age. The reduction in strength of the EPS composite can be explained by the lower specific gravity of EPS, which reduces the concrete's weight but slightly compromises its compressive strength. Nonetheless, the compressive strength of the EPS mixes remains well within the target for Class 20/25 concrete, showing that EPS effectively lowers the weight while maintaining adequate structural integrity.

Water absorption results show that the EPS-added concrete (M2) exhibited a higher absorption rate of 3.2% at 28 days compared to 2.83% for Conventional concrete (M1), due to EPS creating voids within the concrete matrix. As RSF is added, water absorption increases from 3.58% at 0.5% RSF to 5.11% at 1.5% RSF, attributed to RSF's hydrophilic and porous nature, which increases the concrete's porosity and allows more moisture to penetrate.

The inclusion of RSF further improved the tensile and flexural strengths of the composite. This enhancement is due to the fibrous nature of RSF, which bridges cracks and increases the concrete's resistance to tensile and bending stresses by distributing the load more evenly. While the tensile and flexural strengths of Conventional concrete (M1) were sufficient, they were surpassed by those of the composite containing both EPS and RSF. This improved balance between compressive, tensile, and flexural strengths highlights the complementary nature of EPS and RSF in producing effective lightweight concrete.

4.2.3 Proportional Relationship of EPS and RSF and the Performance of Lightweight Concrete

The proportion of EPS and RSF plays a key role in the mechanical performance of lightweight concrete. Increasing RSF content improved tensile and flexural strengths, while compressive strength slightly decreased but remained within acceptable limits. For example, mix M4 (1.0% RSF) had a moderate water absorption of 3.9%, achieved a compressive strength of 27.5 MPa, a tensile strength of 2.65 MPa, and a flexural strength of 3.75 MPa at 28 days. However, in mix M5 (1.5% RSF), water absorption exceeded 5%, indicating potential segregation and reduced cohesion, suggesting that RSF content beyond 1.0% may not be ideal.

The increase in tensile and flexural performance is due to RSF's fibrous structure, which bridges cracks and distributes stress more effectively under bending and tension. In contrast,

the slight reduction in compressive strength, as seen in M5 (27.7 MPa), is attributed to the introduction of voids by organic fibers, which can affect the concrete's density and compactness.

An optimal balance between EPS and RSF is necessary for obtaining the desired mechanical properties in lightweight concrete. The optimal mix in this study was determined to be 10% EPS and 1.0% RSF, which provided a good balance, maintaining sufficient compressive strength while enhancing tensile and flexural properties.

4.2.4 Feasibility and Potential Benefits into Practical Applications

The commercial use of both EPS and RSF in lightweight concrete is substantiated by the results, which demonstrate that the composite has met the target strength for a Class 20/25 concrete. The composite has this advantage mainly because of the EPS embedded in it – less weight. Thus, it is useful in any scenario where weight is an important factor especially in high rise buildings, precast elements or in non-load bearing members. The use of RSF increases tensile and flexural strengths making the composite useful in scenarios where the end product will be exposed to tensile and bending forces such as pavements, slabs, beams.

The mechanical performance improvements are due to the enhancing effects of the EPS and RSF. While EPS is effective in reducing the density of the concrete, RSF improves the matrix by preventing crack growth and redistributing stress under tension and bending load. Even though there was a little decrease in the compressive strength of the samples, the composites are still fit for practical use due to the properties of the composites.

EPS, which is a plastic waste, and RSF which is a waste from the farming environment are both green materials. The combination of these materials not only decreases pollution but also a resource-efficient alternative to conventional concrete components, which uses more resources and is less environmentally friendly. This fits with the new perspective on eco-friendly construction.

5. Conclusions and Recommendations

5.1. Conclusion

1. **Properties of RSF and EPS:** RSF (tensile strength: 4.19 MPa, density: 118.14 kg/m³) enhances ductility and bonding, while EPS (density: 19.7 kg/m³) significantly reduces weight. However, high water absorption rates (RSF: 241.11%; EPS: 94.12%) may necessitate adjustments in the water-cement ratio and the use of superplasticizers.

2. **Composite Performance:** The EPS-RSF composite demonstrated improved tensile and flexural strengths, despite a slight decrease in compressive strength due to increased porosity. This combination enhances structural integrity and durability.
3. **Optimal Mix Ratio:** An optimal mix of 10% EPS and 1.0% RSF balances weight reduction and mechanical performance. Higher RSF content increases water absorption and porosity, adversely affecting cohesion.
4. **Practical Applications:** The EPS-RSF composite is feasible for non-load-bearing structures and prefabricated elements, providing thermal insulation and supporting sustainable construction practices.

5.2. Recommendations

5.2.1. Recommendations from this Study

1. Utilize the EPS-RSF composite in lightweight, crack-resistant construction projects, such as high-rise buildings, with adjustments to the water-cement ratio to enhance workability.
2. Incorporate RSF into EPS-modified concrete to improve tensile and flexural strengths for applications demanding durability, like pavements and non-load-bearing walls.
3. Recommend a mix of 10% EPS and 1% RSF to achieve a favorable balance of density reduction and tensile strength.
4. Promote the adoption of RSF and recycled EPS aggregates to achieve green construction practices.

5.2.2. Recommendations for Further Study

1. Water-Cement Ratio Variations. Consider the different water-cement ratios that would be more beneficial to EPS-RSF composites.
2. EPS and RSF Proportions. Test a wider range of EPS and RSF proportions with regards to strength and durability.
3. Long-Term Durability. Study the durability of the EPS-RSF composite over a prolonged time frame against varying conditions.
4. Alternative Natural Fibres. Investigate the use of other natural fibers like coconut and sisal among others in improving the lightweight concrete structural quality.
5. Evaluation of Fire Resistance. Evaluate the effect of fire on the EPS-RSF composite and suggest the need for fire inhibiting chemicals.
6. Impact Assessments. Carry out the environmental and economic impact of EPS-RSF composite material compared to conventional materials in order to determine their sustainability and cost.

References

- Achaw, O. W., & Danso-Boateng, E. (2021). Cement and Clay Products Technology. In *Chemical and Process Industries* (pp. 135-170). Springer, Cham.
- Adhikary, S. K., & Ashish, D. K. (2022). Turning waste expanded polystyrene into lightweight aggregate: Towards sustainable construction industry—*Science of The Total Environment*, 837, 155852.
- Ahmad, J., Arbili, M. M., Majdi, A., Althoey, F., Farouk Deifalla, A., & Rahmawati, C. (2022). Performance of concrete reinforced with jute fibres (natural fibres): A review—*Journal of Engineered Fibres and Fabrics*, 17, 15589250221121871.
- Aljalawi, N. M. F. (2019). Production of Building Blocks Buffer lightweight Concrete (No. 1510). EasyChair.
- Bede, N., & Malić, N. T. EXPERIMENTAL INVESTIGATION ON LWC WITH COMPLETE REPLACEMENT OF COURSE AGGREGATE BY EPS BEADS.
- British Standards Institution (2009, 2011, 2019, 2021). *Testing hardened and fresh concrete: Tensile splitting strength, water absorption, sampling, slump test, Vebe test, density, compressive strength, flexural strength, and other key properties* (BS EN 12390-1:2021, BS EN 12390-2:2019, BS EN 12390-3:2019, BS EN 12390-4:2019, BS EN 12390-5:2019, BS EN 12390-6:2009, BS EN 12350-1:2019, BS EN 12350-2:2019, BS EN 12350-3:2019, BS EN 12350-4:2019, BS EN 12350-6:2019, BS 1881-122:2011+A1:2020). BSI Standards Publication.
- British Standards Institution (2008, 2011, 2012, 2015, 2020, 2022). *Tests for geometrical properties of aggregates: Determination of particle size, shape, flakiness, percentage of crushed particles, and sand equivalent* (BS EN 933-1:2020, BS EN 933-2:2020, BS EN 933-3:2012, BS EN 933-4:2008, BS EN 933-5:2022, BS EN 933-8:2012+A1:2015). BSI Standards Publication.
- Derman, E., Abdulla, R., Marbawi, H., Sabullah, M. K., Gansau, J. A., & Ravindra, P. (2022). Simultaneous saccharification and fermentation of empty fruit bunches of palm for bioethanol production using a microbial consortium of *S. cerevisiae* and *T. harzianum*. *Fermentation*, 8(7), 295.
- Dianati, K., Schäfer, L., Milner, J., Gómez-Sanabria, A., Gitau, H., Hale, J., ... & Davies, M. (2021). A system dynamics-based scenario analysis of residential solid waste management in Kisumu, Kenya. *Science of the Total Environment*, 777, 146200.
- EN, B. S. (2000). 206-1 Concrete-Part 1: Specification, performance, production, and conformity. British Standards Institution.
- Jiang, D., An, P., Cui, S., Sun, S., Zhang, J., & Tuo, T. (2020). Effect of straw fibre modification methods on compatibility between straw fibres and cement-based materials. *Advances in Civil Engineering*, 2020.
- Lv, C., Liu, J., Guo, G., & Zhang, Y. (2022). The Mechanical Properties of Plant Fibre-Reinforced Geopolymers: A Review. *Polymers*, 14(19), 4134.
- Maghfouri, M., Alimohammadi, V., Gupta, R., Saberian, M., Azarsa, P., Hashemi, M., ... & Roychand, R. (2022). Drying shrinkage properties of expanded polystyrene (EPS) lightweight aggregate concrete: A review. *Case Studies in Construction Materials*, e00919.
- Marcos-Meson, V., Solgaard, A., Fischer, G., Edvardsen, C., & Michel, A. (2020). Pull-out behaviour of hooked-end steel fibres in cracked concrete exposed to wet-dry cycles of chlorides and carbon dioxide—mechanical performance. *Construction and Building Materials*, 240, 117764.
- Moutassem, F. (2020). Ultra-lightweight EPS concrete: Mixing procedure and predictive models for compressive strength. *Civil Engineering and Architecture*, 8(5), 963-972.
- Mudasir, P., & Naqash, J. A. (2021). The effect of water cement ratio on the characteristics of multi-walled carbon nanotube reinforced concrete. *Materials Today: Proceedings*, 43, 3852-3855.
- Mukhdomi, B. A., Reddy, B. A., Keerthana, M., & Murry, L. P. (2021). Experimental Study on Recycled Aggregate-Based Blended Cement Concrete.
- Prasittisopin, L., Termkhajornkit, P., & Kim, Y. H. (2022). Review of concrete with expanded polystyrene (EPS): Performance and environmental aspects. *Journal of Cleaner Production*, 132919.

- Salahaldeen, A. S., & Al-Hadithi, A. I. (2022). The Effect of Adding Expanded Polystyrene Beads (EPS) on the Hardened Properties of Concrete. *Engineering, Technology & Applied Science Research*, 12(6), 9692–9696.
- Sardar, A., Nematy, P., Paskiabi, A. S., Moein, M. M., Moez, H., & Vishki, E. H. (2020). Prediction of mechanical properties of lightweight basalt fibre reinforced concrete containing silica fume and fly ash: Experimental and numerical assessment—*Journal of Building Engineering*, 32, 101732.
- Shang, X., Yang, J., Song, Q., & Wang, L. (2020). Efficacy of modified rice straw fibre on properties of cementitious composites. *Journal of Cleaner Production*, 276, 124184.
- Sheheryar, M., Rehan, R., & Nehdi, M. L. (2021). Estimating CO2 emission savings from ultrahigh performance concrete: a system dynamics approach. *Materials*, 14(4), 995.
- Wasiu, J., & Baba, D. M. (2020). INFLUENCE OF CHEMICAL POLYMER ADDITIVE ON THE PHYSICAL AND MECHANICAL PROPERTIES OF EXPANDED POLYSTYRENE CONCRETE. *Acta Polytechnica*, 60(2), 158-168.

Improving the municipal solid waste storage system for islands with popular tourist sites and remote locations using adept storage systems with ventilation systems

J. N. Mativo¹, M. G. Kim^{2*}, B. O. Alunda³

¹Samgen Project, Republic of Kenya

²Department of fire and Environmental Safety, Keimyung College University, Republic of Korea

³School of Mines and Engineering, Taita Taveta University, Republic of Kenya

*Corresponding author: episode07@naver.com

Article History

Submission Date: 30th October 2024

Acceptance Date: 9th December 2024

Publication Date: 31st December 2024

Abstract

This study investigates the possible benefits islands and remote locations could have by using a ventilation system for municipal solid waste (MSW) collection at their disposal point. The changes in moisture and ash content due to ventilation were examined in two locations with relative humidity of 50% and 70%, respectively, to highlight the expected benefits for the aforementioned regions. This study also examined the changes in gross and net calorific values for mixed fluffy MSW when subjected to ventilation at the aforementioned relative humidities. On Day 1, the gross calorific values of the mixed MSW ranged from 3461 to 4326 kcal/kg, while the net calorific values ranged from 885 to 2320 kcal/kg. Experimental results showed that a 2-3 day ventilation process is sufficient to achieve the threshold moisture content in the MSW. The moisture content at day 1 was 36~62% and decreased when the ventilation time was increased. From day 3 to 5, the changes in moisture content after the ventilation process were marginal. Even though the changes in ash content were minimal, calorific value increased with a decrease in moisture content, such that the critical ventilation period is 2-3 days, after which the MSW exhibited normalized and predictable characteristics irrespective of the cumulative effect. Thus, this study highlights the possible benefits accrued by residents, local municipalities, and waste-to-energy plants using the MSW as fuel.

Keywords: *Municipal solid waste, calorific values, moisture, time series analysis, storage.*

1. Introduction

Municipal solid wastes (MSW) have been a recurrent problem from time immemorial in all countries and are expected to increase by 1.65 times per capita by the year 2050 relative to 2023 [1]. Such an increase is a colossal burden to society, and the federal and/or municipal administrations play an active role in alleviating the problem. Although responsible stakeholders are grasping the nettle to implement sound waste management practices, Maalouf and Mavropoulos [2] observed that one-third of the waste is uncollected, and most of the waste collected is not handled based on established MSW management practices. Thus, the MSW problem will be a recurring issue for some time.

Suffice it to say that high-income countries have strived to establish elaborate municipal solid waste management systems and policies for fast-track collection, sorting/separation, and final disposal [3]. These MSW management systems developed hitherto are focused on urbanized cities and towns with established logistic networks and collection networks understood by stakeholders. On the contrary, islands and isolated areas have geographical limitations [4,5]. These geographic limitations will affect the logistical network necessary for effective MSW collection and disposal. These islands could be tourist and cultural sites or isolated residential areas.

Isolated areas could include regions with makeshift or temporary residential areas for a large workforce working on specialized projects (e.g., oil drilling and exploration, mining, etc.) for a specified period. Islands with important tourist and cultural sites will exhibit increasing, fluctuating, or cyclic MSW generation rates [5,6,7]; it will be challenging to establish a rigid and cost-effective MSW management policy, similar to a large metropolitan city. Also, these isolated islands could be remote and vulnerable to weather changes, hampering the collection and logistics part of MSW [8]. Isolated areas with temporary residential camps may/will not require an established MSW management and disposal system.

Stakeholders have proposed and developed solutions for Island states to alleviate the ever-increasing dangers of open-space garbage dumping and incineration [5-9]. The famous models implemented hitherto are based on waste-to-energy conversion technology since the MSW has considerable calorific values [10]. It is difficult to ascertain the level at which the MSW has been sorted before incineration. Furthermore, the island states have geographic limitations, limiting their capacity to recycle recyclable wastes, e.g., plastics [11]. Thus, if prior sorting of MSW is partially or not implemented at all, then the moisture content is expected to be very high (due to putrescible) and the composition of the incombustible waste (glass, metals, etc.)

to be high. This means that the unsorted MSW will be a source of the unwanted odor and a displeasing feature for the tourist sites in Islands [12,13].

On the other hand, if the unsorted MSW will be incinerated in a waste-to-energy facility, then the net calorific value of the aforementioned MSW will decrease relative to the already sorted RDF. Therefore, modified storage conditions (ventilation) could alleviate the 'moisture' problem in unsorted MSW before incineration by reducing moisture content by approximately 50-70% for MSW with putrescible composition ranging from 50 to 70 wt% [14]. The ventilation solves the problem of unnecessary odours, and such systems could be mobile installations that can be installed anywhere. By implementing ventilation process, the gross calorific value is expected to increase by 15% relative to the original MSW collected and analyzed on an as-it-is basis. Thus, establishing mobile MSW storage containers with partial ventilation could be an optimal method of upgrading the unsorted MSW (if other options are not economically viable) before waste-to-energy conversion.

Generally, MSW in islands and remote locations will be collected and accumulated in trash containers with time, and the MSW collection frequency could be daily or once a week [8]. High moisture load will either remain the same or is expected to increase due to the decomposition of putrescible. Both gross and net calorific value of fuels(i.e., MSW) are heavily dependent on combustible (i.e., carbon) and noncombustible (i.e., moisture, sulfur, ash content) components. Thus, if the moisture content is very high due to decomposition, the gross and net calorific values will eventually decrease. Hence, the need to maintain or upgrade the calorific value is of the essence. As mentioned before, previous research showed that modified storage conditions with ventilation is optimal for storing unsorted MSW before incineration in a waste-to-energy facility and thus solving the unnecessary odor problem, especially in such islands where MSW collection frequency could be several times a week or even once a week [8]. In this manner, the stakeholders involved in MSW collection could effectively prioritize and optimize MSW collection with certainty of the expected MSW quality.

However, it is essential to analyze how the calorific values and moisture content vary based on time series decomposition analysis. Previous experimental analyses were based on a six-day period and a fixed quantity of MSW [12,13]. Weekly MSW accumulation coupled with ventilation will enhance evaporation and partial drying of the MSW such that the putrescible decomposition will be minimal. Thus, this experimental research focused on the effect of ventilation on moisture content and the calorific values of unsorted MSW subjected to continuous MSW accumulation. The material used and respective experimental protocols will be described, and the results obtained will be discussed.

2. Materials and methods

2.1. Materials

Simulated materials (unsorted MSW) were used in this experiment and consisted of putrescible, paper, shredded plastic, woodchips, and soil; the admixture was based on the ratios provided in [12,13] and shown in Table 1. The putrescibles were composed of vegetable wastes. Conventional PVC plastic bags were used, which were shredded together with printed waste papers in a document shredder to match the approximate particle size.

Table 1. Composition of the products used in unsorted MSW preparation

Particulars	Composition, wt. %		
	Set 1	Set 2	Set 3
Putrescible	50	60	70
Paper	20	15	10
Plastic	20	15	10
Wood (sawdust)	5	5	5
Soil	5	5	5

※ Adapted from Nzioka et al. [14, 15]

Products were obtained and used on “as received” basis. In previous experiments, particle size of <20mm was applied; the particle size was determined using the formulations recommended by [16]. The putrescible was chopped to the approximate size. Sawdust was obtained from the local sawmill.

2.2. Experimental setup

After preparation, the components were mixed thoroughly, and the average particle size was confirmed. The sample was mixed using a small animal feed mixing equipment capable of mixing materials with high moisture content. Firstly, soil and sawdust were mixed together with the putrescible waste according to the proportions articulated in Table 1. Later on, the shredded papers and plastic composition were gradually added to the putrescible-soil-sawdust mixture in the mixing equipment to ensure maximum mixing.

The experiment was conducted in an open space with natural ventilation to emulate current MSW trash bin installations. The reactors were placed on a raised level (1,000 mm from ground level) and placed in areas with calm to light air breeze (windspeed up to 19 km/h). The reactor

used was a cubic reactor (500mm length, 500mm width, 700mm height), and the reactor walls were fabricated from polyurethane-coated sheets (Figure 1).

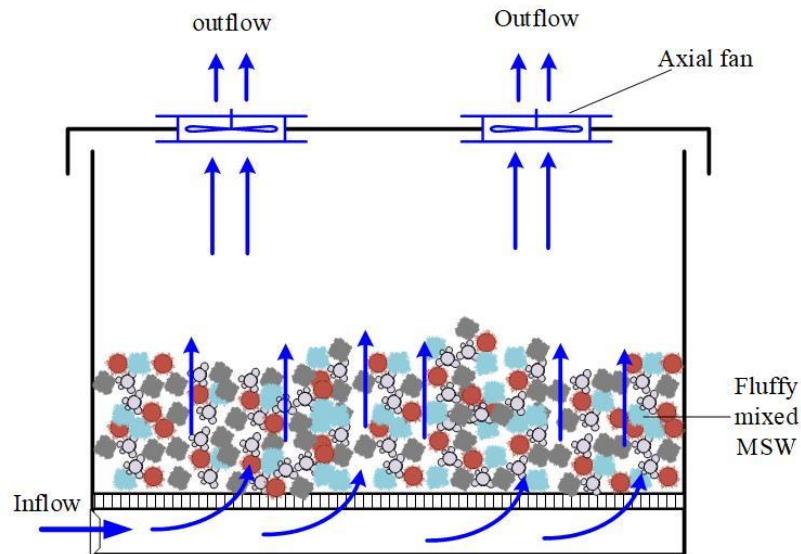


Figure 1. Experimental reactor

The reactor floor was raised by 100mm (Figure 1) to ensure free air flow under the sample. Each reactor ceiling was fitted with two axial ventilation fans (GDSTIME EC brushless fan, 120 mm X 120 mm X 25mm) to create ventilation in the reactor: each ventilator capacity was approximately 2.5 m³/min. The ventilators were fixed on the roof of each reactor. The ventilation cycle for the aeration tank was 15 minutes run/30 minutes stop. Each ventilator’s Cross-sectional areas of the entry and exit chutes were equal (i.e. 36 ± 2cm²). Thus a total of 3 reactors were constructed and used in the two different weather conditions described in the following section.

2.3. Analytical methods

The residual moisture was analysed using the halogen lamp moisture analyzer (XY-101ME). Ash content was analyzed using a muffle furnace at a temperature of 800°C: 3 samples were used to derive the mean ash content. The gross calorific value was determined using an isoperibol oxygen bomb calorimeter (Parr Instruments model 6200): mean gross calorific value was determined from 5 samples. The net calorific values were determined using the formulas used in the previous experiment [14] provided in Table 2. Also, the atmospheric temperature, relative humidity, and dew point were analyzed using a portable thermo-hygrometer placed next to the reactors.

The MSW mass was cumulative in this experiment since 1.5 kg of unsorted mixed MSW was prepared and added daily. On day 1, MSW was sampled before commencing experimental analysis (sample hereinafter termed “Bfr”). After 24 hours, the mixed MSW was poured from

the reactor onto a flat surface covered with plastic sheet to avoid material loss. The material was mixed and lumped for sampling. 100 g was sampled using the quartering sampling method (sampled termed hereinafter “Aft”). After sampling, the existing MSW was mixed with freshly mixed MSW and lumped together for sampling. Later on, 100 g was sampled using the quartering sampling method, after which the sample was poured back into the reactor. The mixed MSW was spread across the reactor bed layer to form a uniform layer.

Table 2. Formulas for calculating net calorific values

Particular	Formula
ASTM E955-88	$Q_n = Q_g \times \frac{[100 - (X + A)]}{100}$
Ilinykh	$Q_n = 4600 - 4A - 51.85X$

※ Ash content (A) and moisture content (X) are expressed in percentage values
 ASTM formula was adapted from [17], Ilinykh’s formula was adapted from [18]

Table 3. Weather conditions for the experimental work

Particulars	Classification	
	70%	50%
Mean daytime temperature (°C)	21 ± 2	25 ± 4
Mean nighttime temperature (°C)	15 ± 2	19 ± 1
Relative humidity (%)	72 ± 7	55 ± 2
Atmospheric pressure (mm. Hg)	764	764

The ventilation experiment was conducted for 24 hours and repeated for 5 days. Firstly, 3 sub samples weighing 5 g from the original 100 g sample mass; the residual moisture content was analyzed from these sub-samples. The remaining 85 ± 1 g sample was dried using the convective dryer (Model DHG-9025) for 24 hours at 55 ± 1°C. A portion of the sample was used to analyze the gross calorific values and the moisture content. The experiment was conducted for five days. Experiments were performed based on two weather conditions described in Table 3.

One-way ANOVA test was conducted using Originlab 2019b. The independent variable in this case was the moisture content, while the dependent variables were both the gross and net calorific values for the three sets of MSW (set 1–3) determined using the formulas shown in Table 2. The objective was to analyse the variance level within and between the three set of samples analysed.

2.4. Limitations of this study

The mean particle size used in this experiment was small. In reality, mixed MSW disposed have large irregular particle sizes. Also, in this study, it was assumed that the ventilation airflow was even throughout the experiment. This study did not consider any possible variation in the inflow and outflow across the cross-sectional area of the reactor. Also, it was assumed that the weather conditions were predictable and that the weather conditions were based on the measurements recorded in the morning and late evening every day. Also, the materials used in the experiments were model MSW, which may differ from one region

3. Results

3.1. Moisture and ash content analysis

Table 4 describes moisture changes due to ventilation at different weather conditions. MSW set 3 had the highest moisture content (60-62%) on day 1 before analysis: the moisture decreased after consecutive ventilation and the addition of freshly mixed MSW (Table 4). on the contrary, MSW set 1 had the lowest moisture content (36-39%), and similar decrease was observed after consecutive ventilation and the addition of freshly mixed MSW. After 24 hour ventilation experiment, moisture content decreased by median value ranging from 45~53% and 50~52% for MSW ventilated at 50% and 70%, respectively.

The first two days of ventilation exhibited a steep decrease in moisture content. The moisture content (Aft) decrease from day three was minimal and showed signs of stability. This could be attributed to the fact that the dominant MSW mass' moisture content is at the minimum level. MSW set 1 decreased from 39.45% (Day 1 Bfr) to 21.44% (Day 1 Aft). Even though the moisture content increased to 32.11%, consequent ventilation reduced the moisture content to 19.84% and similar trend was observed in all case studies. Therefore, the cumulative effect has little influence on the MSW's moisture content after day 3 of ventilation. Also the relative humidity had a negligible impact on the MSW's moisture content.

As for the ash content (Table 5), negligible changes in the ash content of the MSW (i.e samples BFr and Aft) were observed. These negligible changes were similar for the different climatic conditions used in this experiment. The ash content was not affected by the ventilation experiment. The putrescible composition and structure did not change to affect the ash content of the MSW.

Table 4. 5-day moisture content analysis

Humidity level	Type of MSW	Day 1		Day 2		Day 3		Day 4		Day 5	
		Bfr	Aft	Bfr	Aft	Bfr	Aft	Bfr	Aft	Bfr	Aft
70%	Set 1	39.45	21.44	32.11	19.84	31.09	18.24	27.23	17.23	25.29	16.54
	Set 2	51.42	24.78	46.88	21.33	38.26	19.37	37.23	18.76	36.51	18.21
	Set 3	62.34	28.52	51.27	24.69	43.99	21.22	41.8	20.97	41.36	20.86
50%	Set 1	36.52	18.41	31.45	17.65	26.46	15.65	21.84	14.61	21.09	14
	Set 2	49.66	21.82	41.23	18.23	34.87	16.99	29.21	15.84	29.06	15.69
	Set 3	60.86	28.68	48.45	23.1	39.41	19.81	34.21	18.23	31.22	17.14

※ Bfr – before experiment; Aft – after 24 hours experiment

※ Moisture was measured as a percentage of the original material

Table 5. 5-day ash content analysis

Humidity level	Type of MSW	Day 1		Day 2		Day 3		Day 4		Day 5	
		Bfr	Aft	Bfr	Aft	Bfr	Aft	Bfr	Aft	Bfr	Aft
70%	Set 1	8.45	8.95	9.21	8.77	8.96	9.06	8.94	9.24	9.06	9.45
	Set 2	9.87	9.97	9.46	10.21	10.08	9.91	9.65	10.17	9.26	9.91
	Set 3	12.1	11.68	12.18	12.31	11.84	12.02	11.97	12.14	11.84	12.14
50%	Set 1	9.86	10.21	10.84	10.66	10.89	10.61	10.98	11.21	10.45	10.77
	Set 2	10.25	11.12	11.26	11.01	11.26	11.45	11.65	11.87	11.14	11.69
	Set 3	12.93	12.24	12.16	13.14	12.99	12.45	13.26	12.44	13.51	12.96

※ Bfr – before experiment; Aft – after 24 hours experiment

3.2. Calorific values analysis

Table 6 shows changes in gross calorific values during the 5-day experimental period. The initial gross calorific values were 4172 and 4326 kcal/kg for MSW set 1 before experimental analysis at relative humidity of 70% and 50%, respectively. After 24 hours of ventilation, the

gross calorific values increased to 4391 and 4530 and 4326 kcal/kg for MSW set 1 experimented at relative humidity of 70% and 50%, respectively.

After Day 2 of ventilation, the gross calorific values of the samples normalized at the 4400 and 4600 kcal/kg diapason for MSW set 1 experimented at a relative humidity of 70% and 50%, respectively (Table 6). Similar trend was observed for MSW set 2 and 3 at a relative humidity of 70% and 50%, respectively. Ventilation enhances moisture mass transfer together with possible organic chemicals that foster degradation. The fluffy nature of the MSW enhances the mass transfer in-between the layers of the MSW. Thus, day 2-3 are the critical point at which the MSW will maintain stable calorific values.

Table 6. 5-day Gross calorific value (kcal/kg)

Humidity level	Type of MSW	Day 1		Day 2		Day 3		Day 4		Day 5	
		Bfr	Aft	Bfr	Aft	Bfr	Aft	Bfr	Aft	Bfr	Aft
70%	Set 1	4172	4391	4210	4422	4199	4445	4217	4445	4192	4426
	Set 2	3984	4156	4012	4186	3992	4197	4018	4196	4003	4188
	Set 3	3461	3617	3486	3652	3491	3655	3496	3659	3491	3662
50%	Set 1	4326	4530	4369	4610	4315	4631	4354	4625	4362	4631
	Set 2	3728	3921	3735	3962	3733	3965	3754	3961	3719	3952
	Set 3	3537	3710	3615	3785	3650	3821	3647	3819	3648	3799

※ Bfr – before experiment; Aft – after 24 hours experiment

Net calorific values are dependent on the moisture and ash content. Further, the difference between the net calorific results using the two formulas presented in Table 2 was in the range of 331~500 kcal/kg for MSW set 1 and increased to 352~870 kcal/kg for MSW set 2 and 435~1017 kcal/kg for MSW set 3. Such variation could be attributed to the difference in the empirical formulation developed and proposed by ASTM standard and Ilinykh, respectively. After day 1 of ventilation, there was a steep change in the net calorific values, mainly due to the moisture content in the MSW. Cumulative effect of the MSW in the reactor did not influence the net calorific value after ventilation; the critical mass of MSW was reached at day 2-3.

Table 7. 5-day Net calorific value derived using ASTM formula (kcal/kg)

Humidity level	Type of MSW	Day 1		Day 2		Day 3		Day 4		Day 5	
		Bfr	Aft	Bfr	Aft	Bfr	Aft	Bfr	Aft	Bfr	Aft
70%	Set 1	2174	3057	2470	3157	2517	3232	2692	3268	2752	3276
	Set 2	1542	2712	1752	2866	2062	2968	2134	2982	2171	3010
	Set 3	885	2163	1274	2301	1542	2440	1616	2448	1634	2454
50%	Set 1	2320	3234	2521	3305	2703	3415	2925	3431	2986	3484
	Set 2	1495	2629	1774	2804	2011	2837	2220	2863	2224	2870
	Set 3	927	2192	1424	2413	1737	2588	1916	2648	2016	2656

※ ASTM Formula is derived in Table 2

※ Bfr – before experiment; Aft – after 24 hours experiment

Table 8. 5-day Net calorific value derived using Ilinykh's formula (kcal/kg)

Humidity level	Type of MSW	Day 1		Day 2		Day 3		Day 4		Day 5	
		Bfr	Aft	Bfr	Aft	Bfr	Aft	Bfr	Aft	Bfr	Aft
70%	Set 1	2521	3453	2898	3536	2952	3618	3152	3670	3252	3705
	Set 2	1894	3275	2131	3453	2576	3556	2631	3587	2670	3616
	Set 3	1319	3075	1893	3271	2272	3452	2385	3464	2408	3470
50%	Set 1	2667	3605	2926	3642	3184	3746	3424	3798	3465	3831
	Set 2	1984	3424	2417	3611	2747	3673	3039	3731	3049	3740
	Set 3	1393	3064	2039	3350	2505	3523	2773	3605	2927	3659

※ Ilinykh's formula is derived in Table 2

※ Bfr – before experiment; Aft – after 24 hours experiment

4. Discussion

The fluffy material is porous enough to ensure almost free flow of air throughout the reactor. Thus, the ventilation process, which is in part a convective drying process, will partially reduce the moisture content on the surface of the fluffy MSW. The partial reduction of the moisture content was attributed to the convective heat and mass transfer phenomena between air and the fluffy MSW [19, 20]. As a result, the difference in the moisture equilibrium in and on the surface of the fluffy material will result in increased moisture diffusivity from the material to the surface. Nzioka et al. [14, 15] observed that the moisture content could include other organic acids and chemicals present in the putrescibles. Thus, reducing the moisture and the

other degradable organic chemicals enriches the calorific capacity of the fluffy MSW. Another reason associated with the increased drying capacity is the presence of paper in the fluffy MSW. The paper increases the porosity and surface area of the fluffy MSW and has very high moisture sorption characteristics. Therefore, the moisture transfer from the putrescibles to the paper will take place since the paper and the putrescibles are mixed together. Thus, the overall area in contact with the ventilation airflow will increase by at least a factor of two, and the expected drying rate will increase. The calorific value was increased after 24 hours of drying the fluffy MSW. When fresh fluffy MSW was added and mixed with the semi-dried fluffy MSW in day two of the experiment, the overall moisture content in the reactor was reduced while the air-MSW contact area increased due to the increase of the 'paper factor' in the ventilation process. Therefore, the drying effect after day two of the experiment was more evident than on day one. Further addition of fresh fluffy MSW increased the contact area and the overall drying process. It was observed on day 3, ANOVA analysis showed non-significant variance for all sets of MSW analyzed in this experiment with respect to the gross calorific values. As for the net calorific values, the non-significant variation difference is more prevalent between MSW sets 1–3 and sets 2–3.

If the MSW is not dried, the degradation process commences and is expected to intensify with the storage period [15, 21]. Continuous addition/accumulation of the MSW would have exacerbated the degradation process of the putrescibles in the mixed MSW, leading to significant decrease in calorific values and increased odor. It is possible that the degradation process will increase the moisture content beyond the threshold limit after which, it will be uneconomical to use it as a source of fuel.

5. Possible direct and indirect implications for using ventilation to stakeholders

Results show that ventilation could be one of the optimal solutions to the ever-growing MSW problem in islands and remote areas. MSW storage containers with ventilation will alleviate the degradation precursors and the consequential excess odour due to putrescible degradation through aeration. This could be an additional solution to the problem of such tourist islands and remote areas facing challenges with MSW and being unable to address the mixed MSW problem. Results showed that vast moisture content together with other degrading precursors are easily removed via drying.

Results indicate that day 2-3 are the critical phase, after which the overall normalization of MSW characteristics were observed. Normalization of MSW characteristics means that the waste-to-energy facility will have a predictable combustible MSW after collection. Results showed in section 3 showed that the calorific values normalized after day 3 of ventilation. This

means that the MSW could be collected and utilized as fuel after day 3 of ventilation and thus, the waste-to-energy facility will alleviate the challenges of unpredictable calorific values [22]. The waste-to-energy facility could also focus on optimizing the waste-to-energy facilities and adjudicating the appropriate location since they will have predictable fuel resources [23].

Local municipalities could also benefit from this solution, i.e., ventilation of MSW storage. The minor odour problem during ventilation could be neutralized if additional MSW design measures are considered. The municipality administrations will have secured the sanitary condition of the city and will not be worried about whether the residents and tourists will be disciplined enough to segregate waste at the point of collection. If, for example, the municipal regions face challenging logistical issues due to unforeseen events, then the overall sanitary conditions of the MSW could be neutralized through extended storage period: the experimental results showed that after 3-day storage period, the MSW combustion characteristics are normalized. A typical example is Rome (although not an island, but a popular tourist destination), whereby logistical disruptions caused by multiple reasons created worse sanitary conditions [24]. Also, the experimental results showed that ventilation of MSW is not affected by relative humidity and temperature fluctuations. Thus, the local municipalities may not need additional facilities to counter changes in weather conditions.

Conclusion

This study investigated the possible benefits islands and remote locations could have by using a ventilation system for MSW collection at their point of collection. To highlight the expected benefits for the aforementioned regions, the changes in moisture and ash content due to ventilation in two locations with relative humidity of 50% and 70%, respectively was examined. The following conclusions were made:

- 2-3 day ventilation process is sufficient to achieve the threshold moisture content in the MSW;
- Moisture content after day 3 ventilation process was in the range of 15.65~20.22%;
- From day 3 to 5, the changes in moisture content after the ventilation process were marginal;
- Changes in ash content were negligible since the overall inorganic component was similar across the samples used;
- The difference in relative humidity had minimal effect on the moisture and ash content;
- The gross and net calorific values normalized after day 3 and exhibited predictable characteristics irrespective of the cumulative effect;

- The net calorific values gradually increased between day 1 and 2 and normalized after day 3 of ventilation;
- Odour generated was less significant and could be easily alleviated if additional modification are considered on the trash containers.

Thus, the possible benefits accrued by residents, local municipalities, and waste-to-energy plants using the MSW as fuel were described. Results presented herewith have techno-economic and socio-economic value, hence the need for future investigation. Thus future investigations will consider fluctuation in the freshly added MSW, fluctuation in the MSW composition, and possible design modification of the existing MSW collection system.

References

1. UNEP & ISWA (2024). Global waste management outlook 2024 - beyond an age of waste: turning rubbish into a resource,” Nairobi, UNEP.
2. Maalouf, A, & Mavropoulos, A. (2022) Re-assessing global municipal solid waste generation. *Waste Management & Research*, 41(4), 936–947.
3. Roy, D. & Tarafdar, A. (2022). Solid waste management and landfill in high-income countries BT - circular economy in municipal solid waste landfilling: biomining & leachate treatment : sustainable solid waste management: waste towWealth, P. Pathak and S. G. Palani, Eds., Cham: Springer International Publishing, 1–23.
4. Singh, S. J., Elgie, A., Noll, D. & Eckelman, M. J (2023). The challenge of solid waste on Small Islands: proposing a Socio-metabolic Research (SMR) framework. *Current Opinion in Environmental Sustainability*, 62, 101274.
5. Wang, K. C., Lee, K. E & Mokhtar, M. (2021). Solid waste management in small tourism islands: an evolutionary governance approach, *Sustainability*, 13(11), 5896.
6. Wang, Y., Ruiz-Acevedo, A., Rameez, E., Raghavan, V., Hussain, A. & Fei, X. (2023). Toward sustainable waste management in small islands developing states: integrated waste-to-energy solutions in Maldives context. *Frontiers in Environmental Science and Engineering*, 18(2), 24.
7. Mateu-Sbert, J., Ricci-Cabello, I., Villalonga-Olives, E. & Cabeza-Irigoyen E. (2013). The impact of tourism on municipal solid waste generation: The case of Menorca Island (Spain). *Waste Management*, 33(12), 2589–2593.
8. UNEP (2019). Small island developing states. Waste management outlook, Nairobi, UNEP.
9. Agamuthu, T., Masaru, P. (2014). Municipal solid waste management in Asia and the pacific islands. Challenges and strategic solutions, Springer, Singapore.
10. Chen, M. C., Ruijs, A. & Wesseler, J. (2005). Solid waste management on small islands: the case of Green Island, Taiwan. *Resources Conservation and Recycling*, 45(1), 31–47.
11. Mohee, R., Mauthoor, S., Bundhoo, Z. M. A., Somaroo, G., Soobhany, N. & Gunasee, S. (2015) Current status of solid waste management in small island developing states: A review. *Waste Management*, 43, 539–549.

12. Scaglia, B. & Adani, F. (2008). An index for quantifying the aerobic reactivity of municipal solid wastes and derived waste products. *Science of the Total Environment*, 394(1), 183–191.
13. Scaglia, B., Orzi, V., Artola, A., Font, X., Davoli, E., Sanchez, A. & Adani, F. (2011). Odours and volatile organic compounds emitted from municipal solid waste at different stage of decomposition and relationship with biological stability. *Bioresource Technology*, 102(7), 4638–4645.
14. Nzioka, A. M., Hwang, H. U., Kim, M. G., Yan C. Z., Lee, C. S. & Kim, Y. J. (2017). Effect of storage conditions on the calorific value of municipal solid waste. *Waste Management & Research*, 35(8), 863–873.
15. Nzioka, A. M., Kim, M .G., Hwang, H. U., Kim, Y. J. (2019). Kinetic study of the thermal decomposition process of municipal solid waste using TGA. *Waste and Biomass Valorization*, 10(6), 1679–1691.
16. Keey, R. B. (1992). *Drying of loose and particulate materials*. New York: Hemisphere, 1992.
17. ASTM E955 - 88(2009)e1 Standard Test Method for Thermal Characteristics of Refuse-Derived Fuel Macrosamples. Accessed: May 20, 2017. [Online]. Available: <https://www.astm.org/Standards/E955.htm>
18. Ilinykh, G. V. (2013). Evaluation of MSW thermotechnical properties based on its composition. *PNRPU. Applied Ecology and Urban Development*, 3(11), 125–137.
19. Maroulis, Z. B., Kiranoudis, C. T., &Marinos-Kouris D (1995). Heat and mass transfer modeling in air drying of foods,” *Journal of Food Engineering*, 26(1), 113–130.
20. Defraeye, T., & Radu, A. (2017). Convective drying of fruit: A deeper look at the air-material interface by conjugate modeling. *International Journal of Heat and Mass Transfer*, 108, 1610–1622.
21. Zhang, D. Q., He, P. J., & Shao, L. M. (2009). Sorting efficiency and combustion properties of municipal solid waste during bio-drying, *Waste Management*, 29(11), 2816–2823.
22. Tihin, G. L., Mo, K. H., Onn, C. C., Ong, H. C., Taufiq-Yap Y. H. & Lee, H. V (2023). Overview of municipal solid wastes-derived refuse-derived fuels for cement co-processing. *Alexandria Engineering Journal*, 84, 153–174.
23. Ferdoush, M. R., Al Aziz, R., Karmaker, C. L., Debnath, B., Limon, M. H. & Bari A. B. M. M. (2024). Unraveling the challenges of waste-to-energy transition in emerging economies: Implications for sustainability,” *Innovation and Green Development*, 3(2), 100121.
24. Carlo, A, “How Rome’s rubbish problem is attracting wild boar into the Italian capital,” *Euronews*. <https://www.euronews.com/my-europe/2022/05/18/how-rome-s-rubbish-problem-is-attracting-wild-boar-into-the-italian-capital#:~:text=A%20lack%20of%20effective%20alternatives,in%20the%20search%20for%20food>.

Wellhead Steam Turbine Retrofit

L. Muloli*, P. Chege, C. Maiko, A. Wamwaki

Design & Construction (Business Development & Strategy Department), KenGen

*Corresponding Author: Email: lmuloli@kengen.co.ke

Article History

Submission Date: 23rd September 2024

Acceptance Date: 10th November 2024

Publication Date: 31st December 2024

Abstract

This paper evaluates the technical viability of reusing decommissioned stainless steel components from KenGen's Olkaria 1 geothermal power plant as feedstock for manufacturing turbine blades for modular wellhead power plants. A comprehensive Failure Mode and Effects Analysis (FMEA) was performed on failed wellhead turbine blades to identify critical failure mechanisms and inform design modifications. Preliminary results indicated the potential for localized turbine blade production, offering substantial reductions in lead times and costs compared to traditional import-dependent supply chains. This study positions Kenya as a potential front runner in the domestic manufacturing of turbine components for geothermal power generation within the African continent.

Keywords: Geothermal power plant, Stainless Steel, Computer Aided Engineering (CAE), turbine blade, Failure Mode and Effects Analysis (FMEA).

1. Introduction

Africa's burgeoning geothermal energy sector presents a significant opportunity to harness domestic resources for sustainable power generation.

Highlights

Kenya's geothermal power sector is on the cusp of a transformative shift. The rehabilitation of Olkaria 1 geothermal power plant presents a unique opportunity to convert waste into wealth by repurposing decommissioned stainless steel turbine equipment into high-value turbine components.

KenGen's Olkaria 1 Units 1,2 and 3 geothermal power plant, a pioneering facility in African geothermal energy, is undergoing major rehabilitation, while Olkaria 1 Additional Units 4

and 5 are slated for capacity upgrades. Both projects will generate significant quantities of decommissioned stainless steel equipment, including turbine components.

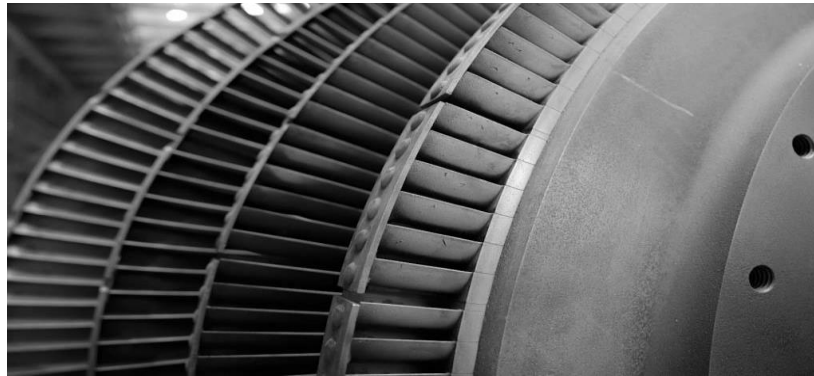


Figure 1. A decommissioned 15 MW Geothermal Steam Turbine Blades at Olkaria 1

Photographed by author, 2024: Courtesy of KenGen PLC)

Highlights

Africa's geothermal energy potential is vast, but its manufacturing capacity for critical components lags behind. This project study aims to bridge this gap by exploring the feasibility of manufacturing turbine blades from decommissioned equipment at KenGen's Olkaria 1 power plant.

Previous research work has explored material repurposing and local manufacturing in various industries, but its application to decommissioned geothermal power plant components remains largely untapped. This study aims to determine if stainless steel from decommissioned Olkaria 1 can be repurposed to create durable turbine blades for wellhead power plants, potentially reducing import reliance and positioning Kenya as a leader in geothermal turbine component manufacturing. Key objectives include demonstrating the feasibility of local turbine component production using indigenous designs, conducting a Failure Mode and Effects Analysis (FMEA) on existing turbine blades to inform design improvements, and assessing the economic and strategic benefits of this approach.

2. Methodology

This study employed a comprehensive approach to analyze turbine blade failures and develop retrofit solutions. Data encompassing operating conditions, material composition, and component geometry were collected from both failed and operational turbines. Metallurgical analyses, including fracture surface evaluation, Nondestructive Evaluation (NDE), microstructure examination, and spectroscopy, were conducted to characterize material properties and failure mechanisms. Computer Aided Engineering (CAE) simulations by Autodesk Inventor, Fusion, ZEISS Blade Inspection, and ANSYS Workbench were employed to assess structural integrity, vibration characteristics, and operational stresses. Concurrently,

an in-depth analysis of operational and steam chemistry data was performed. Additionally, blade profile transformation methods involving melting, casting, barring, and machining were analyzed and modelled using Flow-3D software to inform retrofit.

The integrated findings served as a foundation for proposing retrofit methodologies encompassing blade design optimization, material selection, manufacturing processes, and performance evaluation, all underpinned by cost-benefit analysis and cost-value engineering.

3. Results

Operational parameters of the wellhead turbine were determined as follows: Inlet steam pressure of 13 bar, steam flow rate of 21 tonnes per hour, exhaust steam pressure of 0.1 bar, power output of 2750 kW, and rotational speed of 6804 RPM.

Chemical composition analysis revealed that all turbine blades adhered to the specified chromium content range of 11.5-13.5%. The Wellhead Turbine exhibited the highest average chromium content, while Manganese content was most prevalent in the same turbine. Iron content was predominant in Olkaria 1 Units 1, 2, and 3. The blades from Olkaria 1 Units 4 and 5 demonstrated superior toughness due to higher nickel content and the presence of alloying elements such as vanadium, copper, niobium, and molybdenum. A dearth of data points precluded a comprehensive analysis of steam chemistry. Dimensional inspection and 3D scanning identified defects including blade bending, pitting, and fragmentation, as well as compromised protective coatings. CAE simulations highlighted pronounced stress, vibration, and displacement in the turbine's final stages. Blade profile optimization simulations indicated the potential for vortex reduction and enhanced pressure recovery through angle alterations. However, the necessity for supplementary stress mitigation strategies was evident, with system damping proposed as a potential solution.

```

% Table 1: Wellhead turbine blade chemical composition results
disp('Table 1: Wellhead Turbine Blade Chemical Composition Results - Alloy 410/16/20');
disp('Element      %      ±      SPEC');
disp('Chromium Cr    11.991  0.439  11.5-13.5');
disp('Manganese Mn    0.721   0.126  0.0-1.0');
disp('Iron Fe         86.726  0.436  85.0-88.5');
disp('Nickel Ni        0.4     0.097');
disp('Copper Cu         0.113   0.077');
disp('Niobium Nb        0.039   0.006');
disp(' ');

% Table 2: Olkaria 1 Unit 4&5 turbine blade chemical composition results
disp('Table 2: Olkaria 1 Unit 4&5 Turbine Blade Chemical Composition Results - Alloy 410/16/20');
disp('Element      %      ±      SPEC');
disp('Vanadium V        0.035   0.035');
disp('Chromium Cr       11.926   0.104  11.5-13.5');
disp('Manganese Mn       0.693   0.136  0.0-1.0');
disp('Iron Fe           86.687   0.126  85.0-88.5');
disp('Nickel Ni          0.595   0.132');
disp('Copper Cu           0.03     0.006');
disp('Niobium Nb         0.023   0.016  0.0-0.3');
disp(' ');

% Table 3: Olkaria 1 Unit 1,2&3 turbine blade chemical composition results
disp('Table 3: Olkaria 1 Unit 1,2&3 Turbine Blade Chemical Composition Results - Alloy 410/16/20');
disp('Element      %      ±      SPEC');
disp('Chromium Cr       11.581   0.242  11.5-13.5');
disp('Manganese Mn       0.667   0.271  0.0-1.0');
disp('Iron Fe           87.152   0.382  85.0-88.5');
disp('Nickel Ni          0.397   0.085');
disp('Molybdenum Mo     0.194   0.017  0.0-0.3');
    
```

Figure 2. Chemical Composition Results - Wellhead Units, Olkaria 1 Units 1, 2, 3, Olkaria 1AU 4& 5 - Spectroscopy

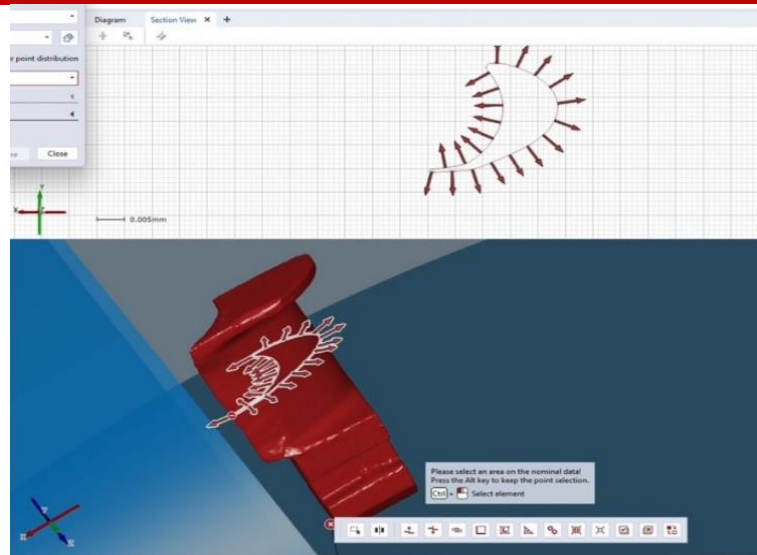


Figure 3. D scanning blade aerofoil inspection - Impala 3D Kenya
Software: ZEISS Blade Inspection - Quality Suite

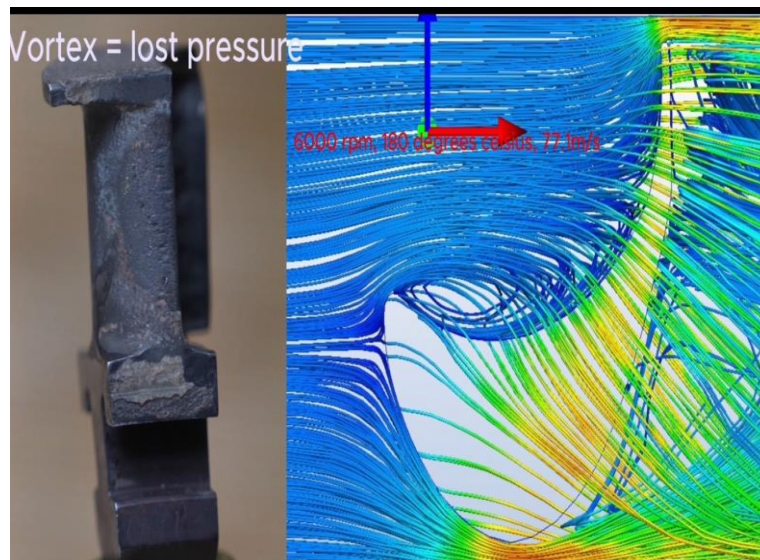


Figure 4. 1st stage blade aerofoil vortex and cavitation points (Indicated by Red) CFD
Software: ANSYS Workbench - Fluent

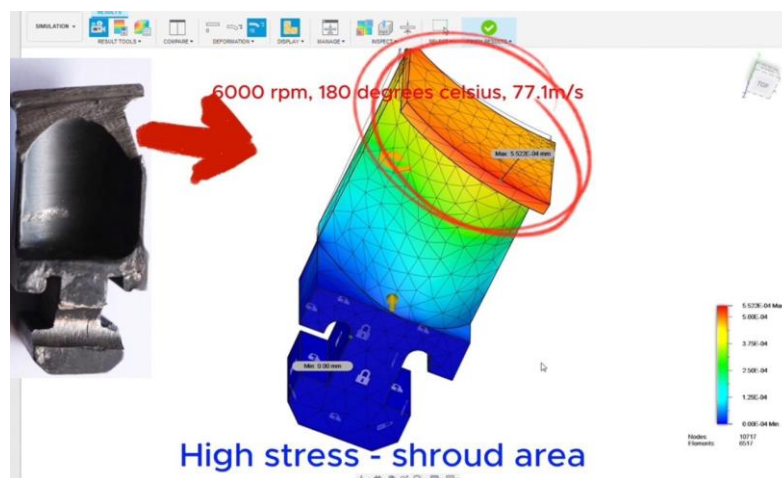


Figure 5. Blade stress analysis - 1st stage
Software: Autodesk Fusion

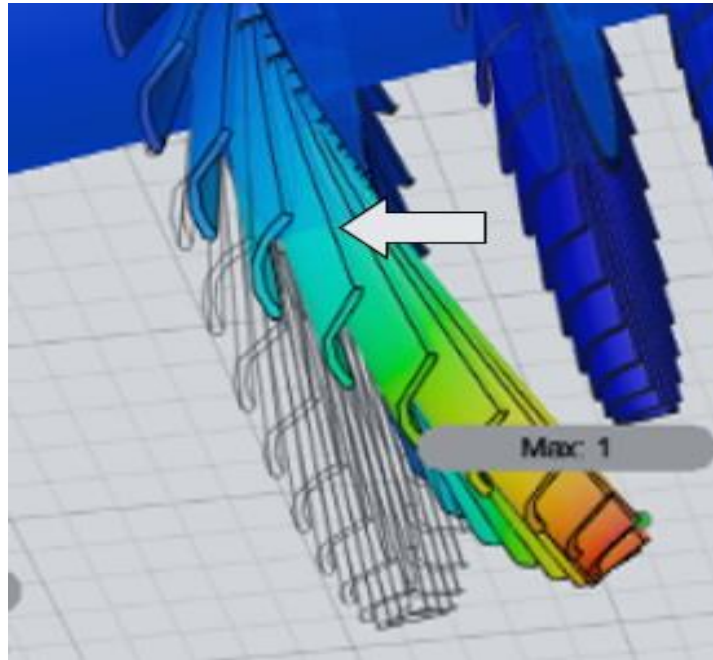


Figure 6. Displacement due to high vibration - 8th stage

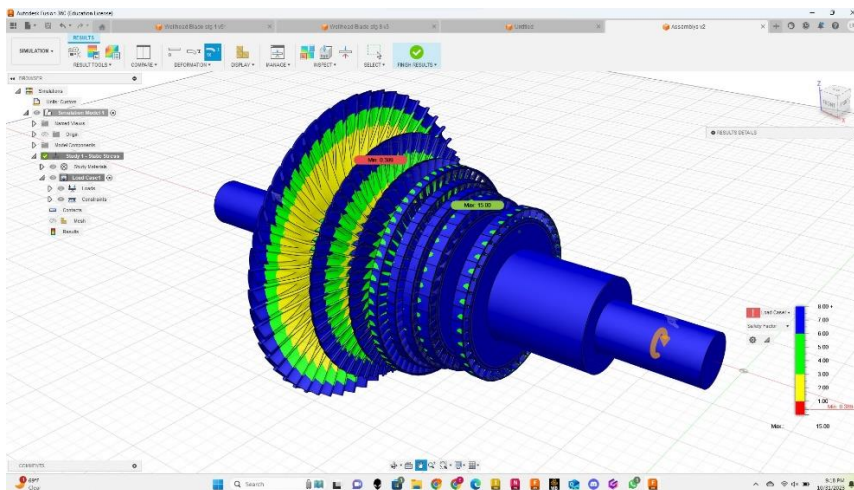


Figure 7. Turbine Rotor Stress Analysis

Software: Autodesk Fusion & Autodesk Inventor

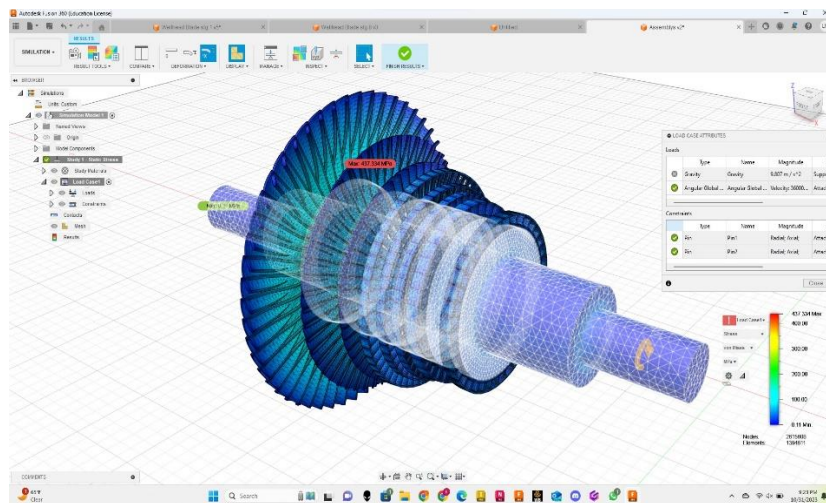


Figure 8. Strain Analysis

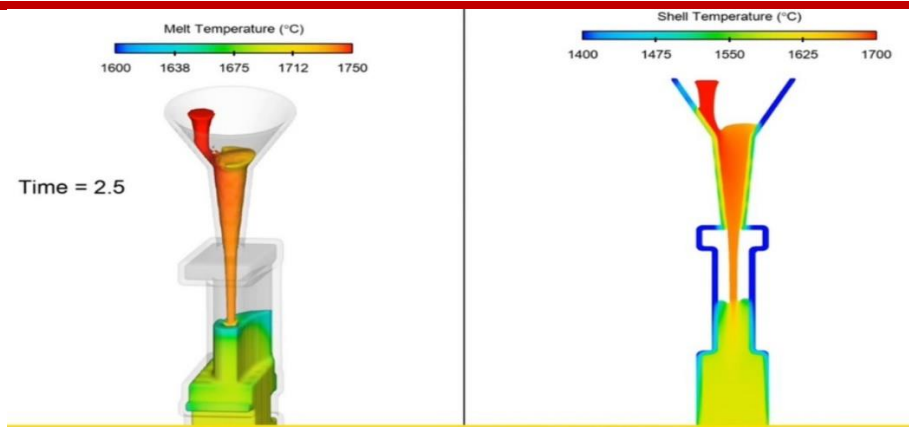


Figure 9. Casting Simulation
Software: Flowcast 3D

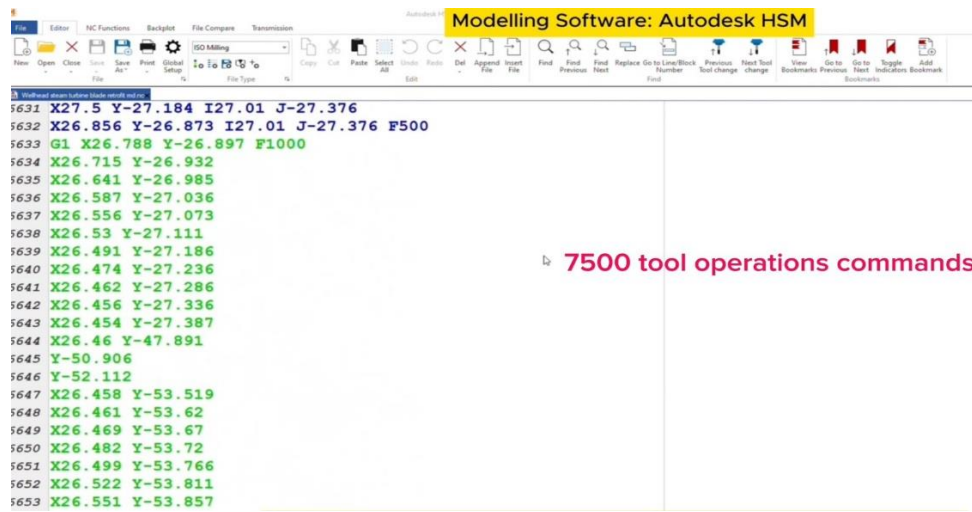


Figure 10. G - Code program Generated snippet - 1st stage Blade
Software: Autodesk HSM

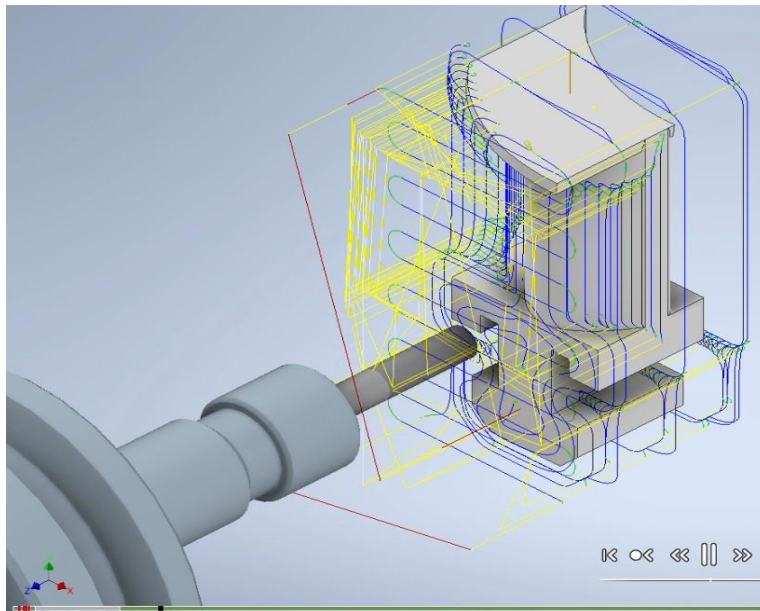


Figure 11. Milling Tool path - 1st stage Blades
Software: Autodesk HSM

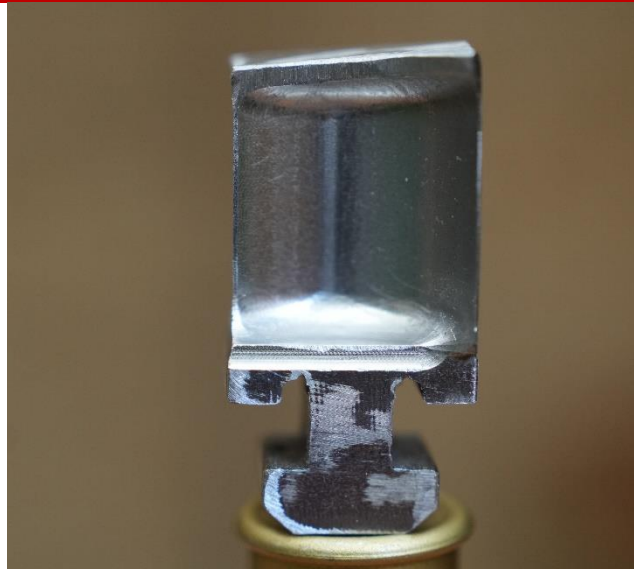


Figure 12. Machined 1st stage Blade Prototype

Manufacturing: DMG MORI 5 Axis CNC Milling Machine - Numerical Machining Complex NMC Ltd. - Kenya

3. Discussions

The operational parameters of the wellhead turbine align with typical values for such systems. However, the observed blade degradation, characterized by bending, pitting, and fragmentation, indicates severe operating conditions or material inadequacies. The identified defects, coupled with the CAE simulations revealing high stress and vibration levels, suggest a complex interplay of factors contributing to premature blade failure.

The chemical composition analysis provides insights into potential material limitations. While all blades met the chromium specification for corrosion resistance, variations in other alloying elements suggest differences in mechanical properties. The superior composition of blades from Olkaria 1 Units 4 and 5, evidenced by higher nickel content and additional alloying elements, highlights the potential for improved performance through material optimization.

The absence of steam chemistry data precludes a comprehensive assessment of its influence on blade degradation. However, given the corrosive nature of geothermal environments, it is plausible that steam impurities contributed to accelerated material deterioration.

The CAE simulations identified critical areas of stress and vibration within the turbine, providing a foundation for targeted design modifications. Blade profile optimization offers potential for performance enhancement but requires further investigation to balance aerodynamic gains with structural integrity. The proposed implementation of system damping is a promising approach to mitigate vibration-induced stresses and extend blade life.

The cost-benefit analysis demonstrated substantial financial advantages of recycling decommissioned stainless steel blades for retrofitting wellhead turbines compared to purchasing new blades or disposing of the blades at scrap value

The study assessed 5100 blades, totaling 21 tonnes, with an initial net value of Ksh 10.5 Billion. Although their current book value is Ksh 330 Million due to depreciation, recycling provides significant cost savings compared to buying new blades.

Auctioning the scrap blades would only yield Ksh 15.2 Million. Recycling these blades incurs costs such as sandblasting (Ksh 3 Million), QA/QC (Ksh 0.1 Million), and machining (Ksh 360 Million), totaling Ksh 370 Million. This recycling cost is substantially lower than the estimated Ksh 630 Million required for new blades, resulting in a cost saving of around Ksh 260 Million.

In comparison, disposing of the blades at their scrap value of Ksh 15.2 Million results in a financial loss when compared to recycling. The recycling process, with its total cost of Ksh 370 Million, still represents a more economical choice than both purchasing new blades and simply disposing of the blades. This analysis highlights that recycling not only saves costs but also optimizes the value derived from the existing materials.

Overall, the findings underscore the need for a holistic approach to address turbine blade failures, encompassing material optimization, improved design, and operational refinements. Further research is warranted to elucidate the specific mechanisms of blade degradation and to validate the proposed solutions through rigorous testing and field trials.

4. Conclusion

The study revealed that the wellhead turbine's operational parameters are within typical ranges for such systems. However, observed blade degradation—characterized by bending, pitting, and fragmentation—indicates severe operating conditions or material deficiencies. CAE simulations further exposed high stress and vibration levels, suggesting a complex interplay of factors contributing to premature blade failure.

Chemical composition analysis identified variations in alloying elements, with blades from Olkaria 1 Units 4 and 5 showing superior properties due to higher nickel content and additional alloying elements. These variations underscore the potential for material optimization to improve performance. The lack of steam chemistry data limits a full assessment of its impact on blade degradation, yet the corrosive geothermal environment likely exacerbates material wear.

The CAE simulations highlighted critical stress and vibration areas, guiding targeted design modifications. Blade profile optimization, while promising, requires further investigation to balance aerodynamic and structural needs. The proposed system damping offers a viable solution to mitigate vibration-induced stresses and extend blade life.

Financially, recycling decommissioned blades proves significantly advantageous compared to purchasing new blades or disposing of them at scrap value. Recycling costs (Ksh 370 Million) are notably lower than the cost of new blades (Ksh 630 Million) and the potential revenue from scrap (Ksh 15.2 Million). This demonstrates that recycling not only provides substantial cost savings but also maximizes the value of existing materials, making it the most economical and beneficial choice for retrofitting wellhead turbines.

5. Recommendations

- 1) Given the compelling economic advantages demonstrated, recycling decommissioned turbine blades should be prioritized as a cost-effective and sustainable solution. To further enhance operational capabilities and unlock new revenue streams, investing in advanced manufacturing technologies is essential. Specifically, acquiring a 5-axis lathe machine would significantly improve machining precision and efficiency, supporting high-quality retrofit operations. Additionally, continuous research, development, and performance monitoring must be integral to these efforts, ensuring ongoing improvements and optimal turbine performance.
- 2) The FMEA results indicate that adjusting the blade angle of attack by -2 degrees can reduce or eliminate vortices and stress breakage, while also increasing pressure harvesting. This adjustment should be integrated into the retrofit process to enhance the overall efficiency and longevity of the turbine blades. Gradual, stage-by-stage manufacturing, proceeding through the eight stages in phases, shall build up the whole turbine rotor incrementally. This approach allows for systematic assessment and refinement at each stage.
- 3) Pioneering engineering manufacturing in Africa through recycling and reverse engineering offers a unique opportunity to develop indigenous design technology. The accuracy of reverse engineering, however, is limited by the applied measurement and computer-aided modelling techniques, such as wear of the part, numerical, sensing, and approximation errors, and manufacturing methods. Turbine blades present challenges due to their complex free-form surfaces. Accurate measurement tools, such as Coordinate Measuring Machines (CMM), are recommended to ensure precision.

- 4) By leveraging these practices, the power sector can enhance its technological capabilities, establish a competitive edge, and reduce reliance on imported technologies. This approach not only drives innovation but also fosters local expertise, creating a foundation for sustainable, home-grown engineering solutions. Embracing these strategies will lead to significant cost savings and operational improvements, positioning Africa as a leader in advanced manufacturing within the power sector.

References

- 1) Chege, P., Bardarson, G., & Richter, A. KenGen's Successful Implementation of a Modular Geothermal Wellhead Strategy. Kenya Electricity Generating Company Ltd., Kenya (KenGen) & Green Energy Geothermal UK Limited (GEG). [Online] Available at: <https://publications.mygeoenergynow.org/grc/1033878.pdf>
- 2) Chege, P. (2018). "The 5MW Pilot plant and 75.6MW WELLHEAD PROJECTS - KenGens Journey to World Class Innovation", pp. 2-3, 5-6.
- 3) Contract between KenGen and GEG. "Design, Supply, Installation & Commissioning of Geothermal Wellhead Turbine Generators at Olkaria", September 2012.
- 4) Ruto, H. (2021). "Performance analysis of geothermal turbine set for well-head power plants: a case study of Olkaria, Kenya". Thesis, Moi University, pp. 35-68. [Online] Available at: <http://ir.mu.ac.ke:8080/jspui/handle/123456789/5196>
- 5) Maingi, G. & Kutswa, C. "KWG12 ROTOR 1st stage repair; static balancing, simulation and rebidding". IEEE PES/IAS PowerAfrica Conference proceedings 2021.
- 6) "Technology Applied in Turbines for Geothermal Plants". Mitsubishi Power, [Online] Available at [<https://power.mhi.com/products/geothermal>]:text=Mitsubishi

Informal Settlements challenges implications on the technical solution design for electricity access

O. A. A. Ezzaldeen^{*1}, A. Muumbo²

¹Politecnico di Milano, 20156, Milan, Italy.

²Technical University of Kenya, P.O Box 52428-00200, Nairobi, Kenya.

*Corresponding Author: Email: omehadi@gmail.com

Article History

Submission Date: 30st October 2024

Acceptance Date: 8th December 2024

Publication Date: 31st December 2024

Abstract

The research studies the obstacles to electrification introduced by the challenges of informal settlements. Focusing on mini-grids as an electrification option, the study provides integrated guidelines on the Comprehensive Energy Solution Planning (CESP) framework to assess and consider the context-specific challenges impact on energy planning. Applied to Kingstone village in Mukuru informal settlement in Nairobi, Kenya, the analysis of the context-specific challenges revealed that these challenges may introduce significant constraints and implications for effective energy production and planning in informal settlements. Energy modelling was the tool to determine the optimized energy mix and dispatch. For the base scenario, which consisted of Solar PV, Batteries, and Diesel generators, the Levelized Cost of Electricity (LCOE) of the system was 0.2083 USD/kWh, and despite it being higher than the main grid LCOE, it was significantly lower than the current electricity costs for Mukuru residents, which is 0.4614 USD/kWh. The energy modelling results indicate that electricity produced by the mini-grid is a viable solution when the main grid extension is unavailable. Additionally, applying different scenarios highlights the inclusion of biogas may yield better outcomes in terms of sustainability. However, electricity distribution lines remain a major challenge in poorly structured and unorganized informal settlements.

Keywords: Informal settlements challenges, Energy Modelling, Mini-grids, Comprehensive Energy Solution Planning, Sustainability, Kenya.

1. Introduction

The proportion of people living in urban areas is projected to increase to 60% by 2030. Currently, about one in four (25%) urban residents experience poor living conditions that adversely affect their health, safety, prosperity, and opportunities [1]. Informal settlements represent a form of urban poverty that is predominantly growing in the world, and they represent a significant challenge for sustainable development. In Sub-Saharan Africa, the slums population accounts for 56.2% of all urban residents [2][3]. As discussed by Brasco and Onori [4] in a systematic literature review. The studies regarding the electrification of informal settlements and slums are comparatively scarce.

Limited and unsustainable access to electricity in informal settlements leads to low well-being indicators and negative impacts on various aspects of life [5][6]. Achieving affordable, reliable, and sustainable energy is particularly challenging in unequal communities like informal settlements [7]. Furthermore, in the context of informal settlements, sustainable development and energy provision through standardized top-down approaches that do not take into account the specific challenges of informal settlements often fail [8][9].

Informal settlements share similarities, but each one presents unique challenges and faces specific barriers to electricity service formalization challenges [10] [11]. Although socio-economic challenges in informal settlements are interrelated and can exacerbate each other, it is essential to identify each challenge independently to accurately assess the primary electrification obstacles it implies. Electricity theft [12] [11], vandalism [13], poor infrastructure and street network [14][15], population instability [15], service affordability [16] and poverty penalty [17] are among the challenges that affect the technical solutions design and electrification success.

Modellers often overlook social aspects due to their non-quantifiable nature and modelling challenges. The oversimplification of the energy model can result in inaccurate and irrelevant outcomes [17]. The solution adopted for this study is supplying electricity through 3rd generation mini-grid. By exploiting mini-grid advantages such as reliability and flexibility [50], the aim of the choice is to evaluate their potential in informal settlements context which is different from remote areas.

This research studies the unique challenges associated with electrification in informal settlements. By identifying the specific challenges from both field campaigns and literature review, the study adopts the Comprehensive Energy Solution Planning (CESP) approach [18] to propose a tailored energy solution. Focusing on the technical solution design, the research

provides integrated guidelines based on the CESP framework, which allowed for a detailed assessment of context-specific challenges and their impacts on the energy planning for informal settlements. The significance of the study is to create an applicable and realistic approach that can be generalized to effectively address the specific needs of informal settlements electrification.

2. Materials and Methods

The analysis follows Comprehensive Energy Solution Planning (CESP), which is an iterative framework consists of a combination of three engineering and social phases each complementing each other. The framework is arranged in a clear and ready-to-use structure, relying on counterfactual analysis complementing traditional energy solutions planning methodologies [18]. Additional guidelines are suggested by the study, and they are integrated in the third phase of CESP methodology. These guidelines aim to provide reliable electricity access planning while accounting for the unique challenges of informal settlements. Informal settlements challenges may introduce constraints and/or implications to the energy production side, assessment and consideration of these constraints and implications are crucial to ensure a more realistic and practical solution design.

The challenges analysis is divided into two parts: challenges assessment and challenges consideration.

Challenges Assessment: is a qualitative assessment of the challenges to set a basis for challenges consideration by forming a cause/effect relationship. It starts by evaluating the challenge presence and then the constraints and implications it introduces.

Challenges Considerations: is to determine and quantify the effect of the present challenges on the power production side following the four steps below;

- 1) Choosing the suitable locations according to these criteria's:
 - *Accessibility.*
 - *Safety.*
 - *Ownership.*
 - *Area Availability.*
 - *Integration to the Main grid.*
- 2) Determining and quantifying the constraints introduced.
- 3) Adjustments/sensitivity analysis for the parameters.
- 4) Scenarios for challenges implications.

Energy modelling through MicrogridsPy [19] was the tool to determine the optimized energy mix for electricity provision, considering the implications derived from the suggested guidelines. Building the electricity demand curve is the starting point for the energy system design and modelling, the demand assessment for this case study was based on data collected by SEEDs and a load curve developed by Brasco & Onori [4]. A yearly growth of 8% was adopted for the base load, this growth was linked to the population growth and introduction of new income generating activities. To complete the system design, firstly, an assessment for the local available energy resources is needed. Secondly, the techno economic parameters of the project and technologies should be determined. These parameters were determined based on relative data from the literature and local market analysis.

3. Results

The results presented are focused on the energy modelling for a case study of Kingstone village. Kingstone village is in the Western borders of Mukuru informal settlement [15], with a population of nearly 20,000 people living in 4911 different households on an area of approximately 7.7 ha according to the last census in 2019 [20]. the current Levelized Cost of Electricity (LCOE) for Mukuru residents is 0.4614 USD/kWh [4].

Table 9. Results of the energy modelling scenarios

Scenario	Components	LCOE USD/kWh
Base Scenario	Solar PV, batteries, and diesel generators as a backup	0.2083
Green Scenario	Solar PV, batteries, and biogas generators as a backup	0.1572
On-Grid Scenario	Solar PV, batteries, diesel generators, and main grid as a backup.	0.1692

The minigrad average LCOE in Kenya is around 0.25 USD/kWh [21].

4. Discussion

Due to overpopulation and high density of the informal settlement, there is no available specific area for minigrad installations. Therefore, the installations will be within the informal settlement residential area. The context challenges analysis reveals that they introduce significant constraints and implications for effective energy planning in informal settlements. The qualitative analysis of the challenges is important for the solution design and planning, it illustrated that biogas production from human waste was not feasible with the current infrastructures. Also, it highlighted that poverty penalty increases the dwellers willing to pay (WTP) for better services in Kingstone, which introduces an opportunity to utilizing a 3rd

generation minigrid for electricity provision although its LCOE is higher than that of the main grid.

The quantitative analysis of Kingstone challenges resulted in direct and indirect implications for the energy modelling. The Solar PV technology power production was constrained to the area of 3,400 m² on the roofs of St. Elizabeth Primary School. Also, the limited available area for the organic waste biodigester was 5 m³, which constrained the biogas production to around 3,041.67 m³/year based on simplest model for biogas production estimation [22]. Another constraint introduced in the context is related to the minigrid layout as technologies should be distributed in the suitable location. To account for electricity theft as a lost revenue, higher values of O&M of the technologies was considered.

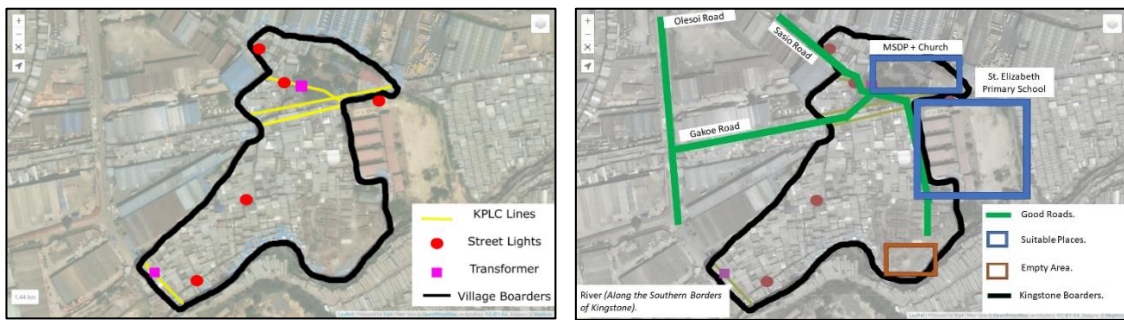


Figure. 1. Spatial analysis of Kingstone.

As electricity demand in informal settlements is only basic needs [8], the dispatch plot of the base scenario highlights the high potential of solar energy to meet demand when supported by batteries, especially during the initial years of the project and periods of high radiation. However, this performance is not sustained throughout the project's entire lifespan due to the increase in demand. This underscores the critical role of backup generators specially when we have a growing electricity demand.

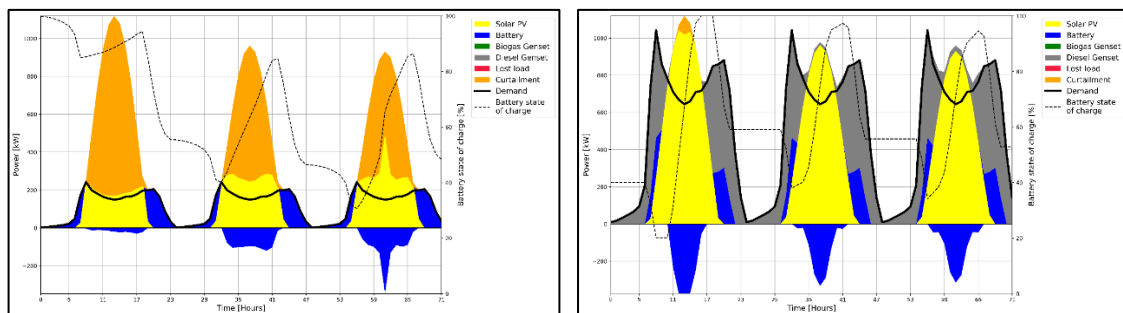


Figure. 2. Optimised Minigrid dispatch on the project first year (left) and last year (right).

The green scenario offers superior economic and social benefits compared to base configurations despite the constraint imposed for the biodigester. Additionally, it is the most

environmentally friendly option as it relies on renewable resources. However, due to the lack of data regarding the characteristics of the available organic waste, suitable assumptions were made to estimate the biogas production and its introduction into electricity generation, but these results remain useful for scenarios analysis as they have impeded data inaccuracy. The integration of the main grid with the base system, which includes Solar PV, BESS, and diesel generators, significantly enhances the overall reliability and economic efficiency of the energy system, but it should be compliant to the regulation and governmental planning, and it introduces system dependency on external energy supply.

5. Conclusions

The study investigates electrification-related challenges to assess the impact of these context-specific challenges on energy planning and electricity production, by proposing and following guidelines integrated into the Comprehensive Energy Solution Planning (CESP) framework.

The challenges of informal settlements in the context of electricity supply should be analysed qualitatively and quantitatively as they may introduce significant constraints and implications for effective energy planning in informal settlements. The constraints imposed by these challenges were resource utilization constraints, area constraints for Solar PV, limited biogas production potential, and mini-grid layout restrictions. Although these challenges imply also considerations for costs such as higher O&M costs, it may introduce business opportunities, such as the poverty penalty which increases the dweller's willingness to pay (WTP) for better services.

For more precise energy modelling, the techno-economic parameters setting was a combination of values from the local market and related literature. The optimized energy mix and dispatch obtained through the modelling indicated that the system LCOE of the base case scenario was 0.2083 USD/kWh, although it is higher than the main grid LCOE of 0.167 USD/kWh, it was less than the average range of mini-grids LCOE in Kenya. The base scenario LCOE remains also competitive for Mukuru dwellers compared to the current LCOE which is 0.4614 USD/kWh due to the relatively high cost of services as a result of the poverty penalty.

Different scenarios were explored; the green scenario and the on-grid scenario. While both offered lower LCOE, the green scenario has an impeded inaccuracy as the data were assumed and were not derived from experiments. The on-grid scenario introduces regulative obstacles and dependency by relying on an external electricity supply. The results suggest that electricity produced by mini-grids is a viable solution for sustainably electrifying informal settlements when the main grid is unavailable.

However, future research should focus on suitable approaches to integrate the economic and social challenges of informal settlements into energy modelling and planning to provide informed results. Additionally, reliable characteristics and parameters of biogas production potential in the area based on experimental and detailed analysis are crucial, given the availability of organic and human waste resources and their high potential to contribute to different aspects of a sustainable solution. Furthermore, electricity distribution lines remain a major challenge in poorly structured and unorganized informal settlements, and further studies on this issue are essential for successful electrification.

References

- [1] Habitat, U. N. "Tracking Progress Towards Inclusive, Safe, Resilient and Sustainable Cities and Human Settlements. SDG 11 Synthesis Report-High Level Political Forum 2018." (2018).
- [2] Klemmer, Konstantin, et al. "Population mapping in informal settlements with high-resolution satellite imagery and equitable ground-truth." *arXiv preprint arXiv:2009.08410* (2020).
- [3] Habitat, U. N. "Metadata on SDGs Indicator 11.1. 1 Indicator category: Tier I." *UN Human Settlements Program, Nairobi* (2018).
- [4] Brasco, Alice, and Alessandro Onori. "electricity access in informal settlements. a case study in nairobi: kingstone, mukuru." (2022).
- [5] G. Frigo, M. Baumann, and R. Hillerbrand, "Energy and the Good Life: Capabilities as the Foundation of the Right to Access Energy Services," *J Human Dev Capabil*, vol. 22, no. 2, pp. 218–248, 2021, doi: 10.1080/19452829.2021.1887109.
- [6] P. J. Lloyd, "The role of energy in development," *Journal of Energy in Southern Africa*, vol. 28, no. 1, pp. 54–62, 2017, doi: 10.17159/2413-3051/2017/v28i1a1498.
- [7] S. Smit, J. K. Musango, and A. C. Brent, "Understanding electricity legitimacy dynamics in an urban informal settlement in South Africa: A Community Based System Dynamics approach," *Energy for Sustainable Development*, vol. 49, pp. 39–52, Apr. 2019, doi: 10.1016/j.esd.2019.01.004.
- [8] P. Njoroge, A. Ambole, D. Githira, and G. Outa, "Steering energy transitions through landscape governance: case of mathare informal settlement, Nairobi, Kenya," *Land (Basel)*, vol. 9, no. 6, pp. 1–19, Jun. 2020, doi: 10.3390/land9060206.
- [9] S. Smit, J. K. Musango, Z. Kovacic, and A. C. Brent, "Conceptualising slum in an urban African context," *Cities*, vol. 62, pp. 107–119, Feb. 2017, doi: 10.1016/j.cities.2016.12.018.
- [10] Z. Kovacic et al., "Interrogating differences: A comparative analysis of Africa's informal settlements," *World Dev*, vol. 122, pp. 614–627, Oct. 2019, doi: 10.1016/j.worlddev.2019.06.026.
- [11] Lemaire, Xavier, and Daniel Kerr. "Informal Settlements-Electrification and Urban Services." (2016): 1-28.

- [12] E. C. X. Ikejemba and P. C. Schuur, "Analyzing the impact of theft and vandalism in relation to the sustainability of renewable energy development projects in Sub-Saharan Africa," *Sustainability (Switzerland)*, vol. 10, no. 3, Mar. 2018, doi: 10.3390/su10030814.
- [13] Appiah-Kubi, Jamal. "Challenges Encountered in community development in urban slums: A study of Ashaiman, Ghana." *International Journal of Science: Basic and Applied Research* 42.1 (2018): 81-93.
- [14] R. Besner, K. Mehta, and W. Zörner, "How to Enhance Energy Services in Informal Settlements? Qualitative Comparison of Renewable Energy Solutions," *Energies (Basel)*, vol. 16, no. 12, Jun. 2023, doi: 10.3390/en16124687.
- [15] Corburn, J., et al. "Situational analysis of Mukuru Kwa Njenga, Kwa Reuben & Viwandani." *Technical paper* (2017).
- [16] Selokela, Bikkie R., and Kristy E. Langerman. "Challenges in electrifying informal settlements: Case study of the 'mixed energy' solution in Thembelihle." *2019 International Conference on the Domestic Use of Energy (DUE)*. IEEE, 2019.
- [17] D. Süsser et al., "Why energy models should integrate social and environmental factors: Assessing user needs, omission impacts, and real-word accuracy in the European Union," *Energy Res Soc Sci*, vol. 92, Oct. 2022, doi: 10.1016/j.erss.2022.102775.
- [18] E. Colombo, G. Crevani, N. Stevanato, and R. Mereu, "Comprehensive energy solution planning (CESP) framework: an evidence-based approach for sustainable energy access projects in developing countries," *Environmental Research Letters*, vol. 19, no. 5, p. 054059, May 2024, doi: 10.1088/1748-9326/ad41ef.
- [19] MicroGridsPy Version 2.1, <https://microgridspy-documentation.readthedocs.io/en/latest/>, Last accessed 2024/03/02.
- [20] Field notes from Nairobi, Kenya, <https://globalchangeecology.com/2022/08/18/field-notes-from-nairobi-kenya/>, last accessed 2024/09/01.
- [21] Energy Sector Management Assistance Program. *Mini grids for half a billion people: Market outlook and handbook for decision makers*. World Bank, 2019.
- [22] Wu, Anthony, et al. "A spreadsheet calculator for estimating biogas production and economic measures for UK-based farm-fed anaerobic digesters." *Bioresource Technology* 220 (2016): 479-489.

Evaluating the Effectiveness of Pumice on Polyvinyl Chloride (PVC)-Treated Red Coffee Soil for Subbase Construction

C. D. Anyango¹, M. W. Kibe², J. N. Thuo³

¹Department of Civil Engineering, Dedan Kimathi University of Technology, Kenya.

Corresponding Author: Email: charitydiana84@gmail.com

Article History

Submission Date: 14th October 2024

Acceptance Date: 4th December 2024

Publication Date: 31st December 2024

Abstract

There is an aim of optimizing the use of local materials of marginal quality for pavement layers like subbase to reduce the total road construction costs significantly. The use of weak and expansive soils for road construction affects the performance and overall behaviors of the entire pavement structure. Stabilization of these weak soils in situ may be done with PVC waste and pumice powder to save on construction costs. The disposal of polyvinyl chloride (PVC) plastic threatens public health and the environment, as discarding PVC waste poses perpetual hazards. The study aimed at reducing harm from PVC by diverting PVC waste away from incineration and open burning into road subbase stabilization. Pumice is an amorphous foam made through volcanic eruptions. It's composed principally of oxide and aluminum in relative amounts. It's a pozzolan which, when reacted with calcium hydroxide in lime at room temperature, forms cementitious compounds. This research determined the effects of pumice as a reinforcement on polyvinyl chloride-treated red coffee soil for subbase construction. The investigation included laboratory tests and analysis of results from the tested samples. The PVC was added in a 1.5% proportion of the dry weight of the soil. The pumice was added in 20%, 30%, 40%, and 50% proportions of the dry weight of soil. The highest MDD and CBR were obtained at 40% pumice proportions, being 1531 kg/m³ and 23.94, respectively. The research concluded that the addition of pumice to the soil sample for subbase construction improves the engineering properties and stability of the pavement layer.

Keywords: PVC waste, pumice powder, subbase construction, weak soils, MDD, CBR.

1. Introduction

The scarcity of traditional road construction materials has led to the exploration of alternatives like plastic waste for soil stabilization (Bu et al., 2019). Red coffee soil, commonly found in Kenya, presents engineering challenges such as high plasticity, swelling, and low bearing capacity, making it unsuitable for road construction without stabilization (Okwadha & Nyingi, 2016). This study focuses on using locally available PVC waste and pumice to stabilize this soil, offering a cost-effective and environmentally friendly solution. Pumice, a pozzolanic material, reacts with calcium hydroxide to improve soil strength and reduce permeability (Mesfun et al., 2019). By incorporating PVC waste and pumice, this research aims to enhance the subbase properties of red coffee soil, providing an economical alternative to traditional methods like cement and lime, which are becoming more expensive (Naturinda, 2021).

2. Literature Review

Research Soil stabilization aims to improve the engineering properties of soil through physical, chemical, or mechanical means. Additives such as lime, which is mainly composed of calcium oxide, enhance soil strength, volume stability, and reduce swelling and shrinkage, especially in soils like Kenya's red coffee soil, which can exhibit low bearing capacity (Okwadha & Nyingi, 2016). Stabilizing these high-plasticity soils is essential to avoid construction problems such as differential settlement and increased project costs.

Plastic waste, particularly PVC, has shown promise in improving soil properties. Studies have found that mixing plastic with soil increases strength and decreases maximum dry density (Abukhattala, 2021). Pumice, a porous volcanic rock, further enhances compressive strength and CBR values when added to stabilize soils (Mesfun et al., 2019). However, further research is needed to optimize the use of powdered PVC in soil stabilization and fully understand its performance when mixed with other materials (Abukhattala, 2021).

3. Methodology

The study tested the engineering properties of expansive red coffee soil treated with pumice powder (0%, 20%, 30%, 40%, and 50% by weight). Tests included wet sieve analysis, Atterberg limits, moisture-density relationship (compaction), and California Bearing Ratio (CBR).

3.1. Materials sourcing and Equipment used

Raw materials were: PVC sourced from dumpsites in King'ong'o, washed and grounded into powder as illustrated in figure 3.1a. Pumice stones were obtained along rift valley escarpment

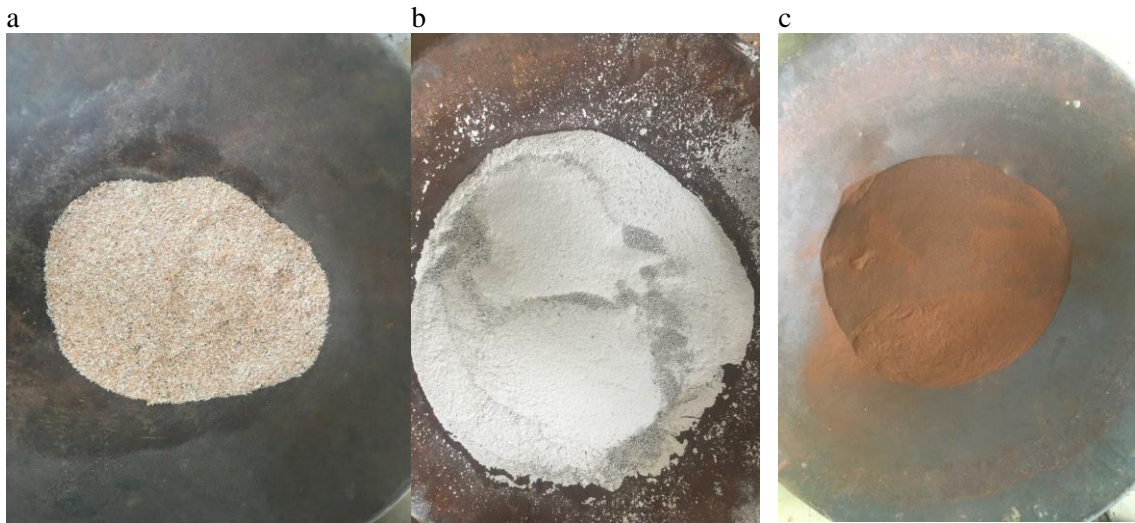


Figure 3.1. Raw materials

Key laboratory equipment included plasticity index apparatus, moisture tins, Atterberg limits apparatus, standard sieves, and CBR apparatus.

3.2. Laboratory Tests

Moisture content: was established per ASTM D-2216 standards (ASTM, 2019). Soil specimens were dried in an oven at 100–110°C for 18-24 hours before testing.

Physical properties: were assessed using gradation and Atterberg limits analyses. Grading followed AASHTO standards, grain size distribution was assessed according to ASTM D422 (ASTM, 2017a), and Atterberg limits were tested per ASTM D4318 (ASTM, 2017b).

The Proctor test: determined the optimal moisture content for maximum dry density (MDD) of PVC-treated red coffee soil, following ASTM D-1557 standards (ASTM, 2021b).

Unconfined compressive strength (UCS) testing, per ASTM D-2166 standards (ASTM, 2016), measured the compressive strength of neat soil, producing a stress-strain curve.

The CBR test: assessed soil strength by measuring resistance to penetration under controlled conditions. Specimens were prepared based on optimal moisture content and MDD, following ASTM D-1883 standards (ASTM, 2021a), with CBR values obtained at 2.5 mm penetration.

4. Results And Discussion

4.1. Results

Table 4.1 shows that the red coffee soil is classified as expansive clay, with key properties indicating a need for improvement to meet engineering standards.

Table 4.1 Properties of Neat Red Coffee Soil

PROPERTY	QUANTITY
Colour	red-brown
Percentage passing No. 200 sieve, %	76.35
Specific gravity	2.62
Void ratio (e)	0.43
Plastic index, %	40.0
AASHTO Soil classification	A-7
Free swell, %	0.646
Maximum dry density, kg/m ³	1301.7
Optimum moisture content, %	40.5
Soaked CBR value, %	1.924
Hydraulic conductivity cm/s	0.01782
Unconfined Compression Strength, qu KN/m ²	38.11
Shear strength qu/2	19.05

The results of the engineering properties of the samples are as illustrated in table 4.2 and in figures 4.1, 4.2 and 4.3

Table 4.2 Soil Sample Test Results Summary

Description	Liquid Limit (LL)	Plastic Limit (PL)	Plasticity Index (PI)	Maximum Dry Density (MDD) kg/m ³	Optimum Moisture Content (OMC) %	California Bearing Ratio (CBR)
Red coffee soil (RCS)	66.5	26.5	40.0	1301.70	40.50	1.924
RCS + 1.5% PVC	63.94	31.23	32.71	1280.00	49.75	3.574
RCS + 4% Lime	64.04	48.0	16.04	1326.16	32.66	19.24
RCS + 1.5% PVC, 4% Lime + 20% Pumice	62.68	47.50	15.18	1376.20	25.67	22.44
RCS + 1.5% PVC, 4% Lime + 30% Pumice	61.32	47.01	14.31	1470.20	22.89	23.74
RCS + 1.5% PVC, 4% Lime + 40% Pumice	57.35	47.11	10.24	1531.00	20.10	23.94
RCS + 1.5% PVC, 4% Lime + 50% Pumice	63.50	49.80	13.70	1501.20	22.00	23.44

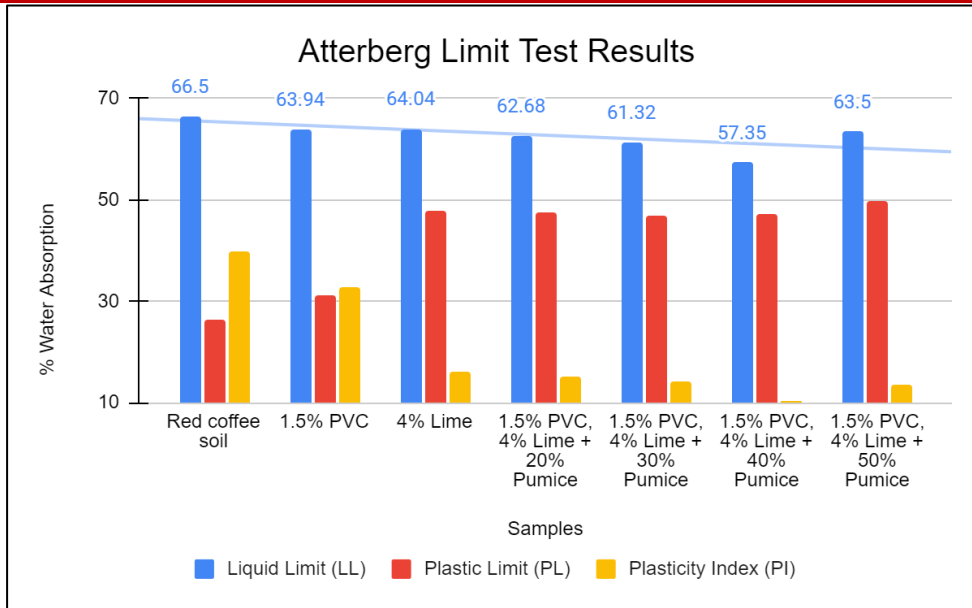


Figure 4.1 Atterber limits

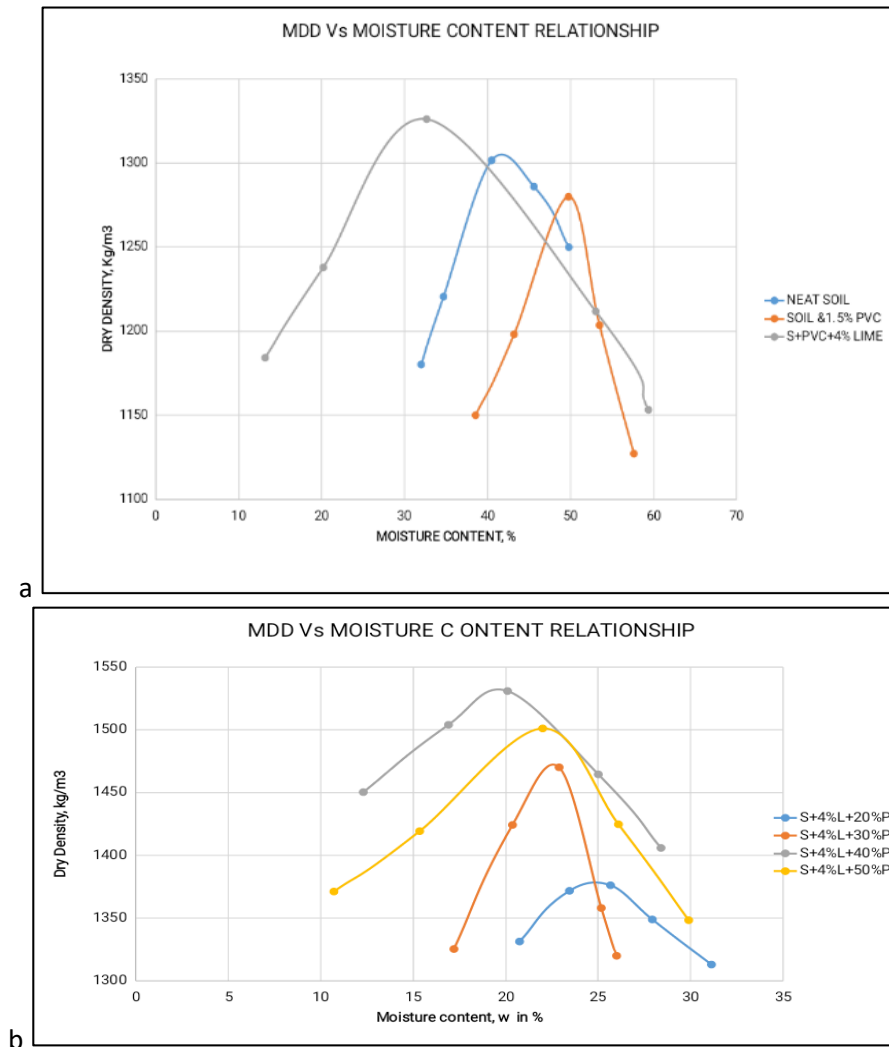


Figure 4.2 a and b Maximum Dry Density

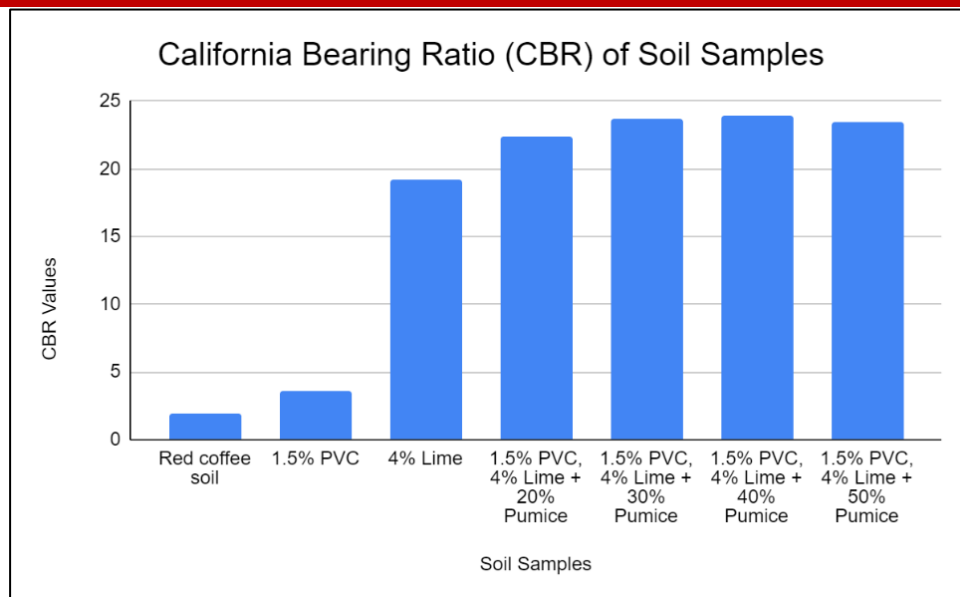


Figure 4.3 California bearing Ratio of various soil samples

4.2. Discussion

4.2.1. Physical and Engineering Properties of Red Coffee Soil

The Atterberg limits test results in table 4.2 and figure 4.1 showed that the red coffee soil had a liquid limit of 66.5%, a plastic limit of 26.5%, and a plasticity index of 40.0%, indicating high plasticity per ASTM D424 standards. This high plasticity suggests potential challenges in construction, as it may lead to deformation and instability under load. The Proctor test revealed a maximum dry density of 1301.7 kg/m³ at an optimum moisture content of 40.5%, emphasizing the importance of moisture management to achieve proper compaction and structural integrity. The CBR test yielded a value of 1.924, highlighting the soil's potential for subgrade applications, though further enhancement may be needed to meet higher load-bearing standards.

4.2.2. Optimum Proportion of Pumice on PVC Treated Red Coffee Soil

The variation of the proportions of the pumice on the PVC treated soil sample had a general decrease in the liquid limit and plasticity index in all the Soil-PVC-Pumice lime combinations. The Plasticity Index of the soil sample decreases drastically, due to its tendency to swell and shrink. After initial mixing, the calcium ions Ca²⁺ from hydrated lime migrate to the surface of the clay particles and displace water and other ions. The soil becomes friable and granular, making it easier to work and compact. The liquid limit decreased to 57.35% and an increase of the plastic limit to 47.11% giving optimum values at 40% pumice. The results are as displayed in Table 4.2 and figure 4.1.

The optimum proportion of pumice in PVC treated RCS was found to be at 40% for proctor test. It was observed that the value of Maximum Dry Density of PVC treated RCS increased with increasing percentage of pumice with a margin up to 19.61%. The MDD increased from 1280kg/m³ to 1531kg/m³ and the corresponding OMC was at 20.10% which was a decrease from 49.75% as displayed in Table 4.2 and figure 4.2a and b. However, a reduction of MDD was noticed at 50% pumice. The increase in MDD may be attributed to high specific gravity of pumice powder.

The increase in MDD showed that pumice powder and lime facilitated in binding up of the particles of the PVC treated soil thus increasing its density. Increasing MDD also indicated reduced permeability and settlement of the soil. Flocculation and agglomeration occurred where; hydrated lime and pumice mixed with PVC treated RCS particles slowly producing drying because they reduce the soil's moisture holding capacity. Drying occurred through the chemical changes in the soil that reduced its capacity to hold water and increase its stability. As illustrated in Table 4.2 and figure 4.3, at 40% pumice proportion, the CBR value increased to 23.94. Values beyond 40% pumice showed a decrease in the values of the different parameters: plasticity index, Maximum Dry Density and CBR.

4.2.3. Strength Contribution of Pumice on Red Coffee Soil

The CBR value for the 1.5% PVC-treated soil was found to be 3.574. Results in Table 4.2 and Figure 4.3 showed a 56.9% increase in the CBR of PVC-treated Red Coffee Soil with added pumice. This demonstrated a significant enhancement in load-bearing capacity due to pumice and lime treatment. The increase in CBR was linked to the formation of cementitious compounds, such as calcium-silicate-hydrates (CSH) and calcium-aluminate-hydrates (CAH), from the calcium in lime and the silica and alumina from the soil and pumice. These compounds, similar to those in Portland cement, formed a matrix that contributed to the strength of stabilized soil layers. The pozzolanic reaction between lime, soil, and pumice led to more cementitious compound formation, while the rise in Maximum Dry Density improved the soil's shear strength and bearing capacity by increasing frictional resistance. The combination of pumice and lime strongly improved the strength of expansive soils.

5. Conclusion, and Recommendation

5.1. Conclusions

- 1) **Properties of Red Coffee Soil (RCS):** RCS has a high liquid limit (66.5%) and plasticity index (40%), indicating its expansive nature. With a low Maximum Dry Density (MDD) of 1301.7 kg/m³ and California Bearing Ratio (CBR) of 1.924, it is

unsuitable for direct pavement applications without stabilization, emphasizing the need for effective stabilization techniques.

- 2) **Optimal Pumice Proportion:** An optimal pumice proportion of 40% by dry weight of soil was identified, reducing the plasticity index by 68.59% and improving workability and compaction. This mix enhances engineering outcomes, increasing the soil's suitability for subbase construction.
- 3) **Strength Contribution and Implications for Construction:** The combination of PVC, 40% pumice, and lime increased the Maximum Dry Density (MDD) to 1531 kg/m³, surpassing the minimum requirement of 1400 kg/m³ outlined in the Road Design Manual Part III. While pumice alone does not strengthen the soil, its reaction with calcium hydroxide in lime produces cementitious compounds due to reactive forms of alumina and silica, which enhance soil strength. The California Bearing Ratio (CBR) improved to 23.94, indicating a significant increase in load-bearing capacity. This highlights the potential of stabilized Red Coffee Soil (RCS) for use in road projects, contributing to the development of more durable infrastructure.

5.2. Recommendations from this Study

- 1) Red Coffee Soil is technically and economically unviable for pavement construction unless stabilized.
- 2) A mix of pumice and lime should be considered for stabilizing PVC-treated Red Coffee Soil, as this combination improves the soil's strength and meets road construction requirements.
- 3) An economic analysis should be conducted to assess the cost-effectiveness of using pumice for road stabilization in large-scale projects.

5.3. Recommendations for Further Study

- 1) Conduct pilot road construction projects using PVC-treated Red Coffee Soil stabilized with pumice and lime to assess field performance and long-term durability compared to laboratory results.
- 2) Investigate alternative pozzolanic materials in combination with lime for further improving the engineering properties of expansive soils in road construction.
- 3) Explore the environmental impacts and sustainability of large-scale pumice mining and its long-term effects when used as a stabilizer in road construction materials.

References

- Abbasi, N., & Mahdiah, M. (2018). Improvement of geotechnical properties of silty sand soils using natural pozzolan and lime. *International Journal of Geo-Engineering*, 9(1). <https://doi.org/10.1186/s40703-018-0072-4>
- Abukhattala, M. (2021). Potential Use of Plastic Waste Materials in Pavement Structures Applications. <https://ruor.uottawa.ca/handle/10393/41762>
- ASTM. (2017a). Standard Test Method for Particle-Size Analysis of Soils. <https://www.astm.org/d0422-63r98.html>
- ASTM. (2017b). Standard Test Methods for Liquid Limit, Plastic Limit, and Plasticity Index of Soils. <https://www.astm.org/d4318-10e01.html>
- ASTM. (2019). Standard Test Methods for Laboratory Determination of Water (Moisture) Content of Soil and Rock by Mass. <https://www.astm.org/d2216-10.html>
- ASTM. (2021a). Standard Test Method for California Bearing Ratio (CBR) of Laboratory-Compacted Soils. <https://www.astm.org/d1883-21.html>
- Bu, F., Liu, J., Bai, Y., Kanungo, D. P., Song, Z., Kong, F., & Pan, C. (2019). Effects of the Preparation Conditions and Reinforcement Mechanism of Polyvinyl Acetate Soil Stabilizer. *Polymers*, 11(3), 506. <https://doi.org/10.3390/POLYM11030506>
- Mesfun, R. T., Quezon, E. T., & Geremew, A. (2019). Experimental study of stabilized expansive soil using pumice mixed with lime for subgrade road construction. *International Journal of Research - GRANTHAALAYAH*, 7(7), 118–124. <https://doi.org/10.29121/GRANTHAALAYAH.V7.I7.2019.736>
- Naturinda, D. N. (2021). Practical Application of Natural Pozzolans and Lime for Cost Optimisation in Low-Cost Housing. *Advances in Science, Technology and Innovation*. https://doi.org/10.1007/978-3-030-48465-1_46
- Okwadha, G. D. O., & Nyingi, P. W. (2016). Effectiveness of rice husk ash in stabilizing Kenyan red coffee soil for road subgrades construction. *International Journal of Environmental Science and Technology*, 13(11), 2731–2734. <https://doi.org/10.1007/s13762-016-1092-2>

Editorial Committee

Name	Category	Country
Eng. Prof. Lawrence Gumbe	Chair	Kenya
Eng. Prof. Leonard Masu	Secretary	Kenya
Eng. Prof. Ayodeji Oluleye	Member	Nigeria
Eng. Dr. Slah Msahli	Member	Tunisia
Eng. Prof. Bernadette W. Sabuni	Member	Kenya
Prof. Anish Kutien	Member	South Africa

Editorial Board

Name	
Chairperson:	Eng. Prof. Lawrence Gumbe
Members:	Eng. Paul Ochola- Secretary
	Eng. Sammy Tangus- Treasurer
	Eng. Erick Ohaga – IPP, IEK
	Eng. Shammah Kiteme- President, IEK
	Eng. Prof. Leonard Masu
	Eng. Margaret Ogai
	Eng. Nathaniel Matalanga
	Eng. Dr. Samwel Roy Orege – Technical Editor

INSTRUCTIONS TO CONTRIBUTORS

The editorial staff of the AJERI requests contributors of articles for publication to observe the following editorial policy and guidelines accessible at <https://www.iekenya.org/> in order to improve communication and to facilitate the editorial process.

Criteria for Article Selection

Priority in the selection of articles for publication is that the articles:

- a. Are written in the English language
- b. Are relevant to the application relevant of engineering and technology research and Innovation
- c. Have not been previously published elsewhere, or, if previously published are supported by a copyright permission
- d. Deals with theoretical, practical and adoptable innovations applicable to engineering and technology
- e. Have a 150 to 250 words abstract, preceding the main body of the article
- f. The abstract should be followed by a list of 4 to 8 "key Words"
- g. Manuscript should be single-spaced under 4,000 words (approximately equivalent to 5-6 pages of A4-size paper)
- h. Are supported by authentic sources, references or bibliography

Rejected/Accepted Articles

- a. As a rule, articles that are not chosen for AJERI publication are not returned unless writer (s) asks for their return and are covered with adequate postage stamps. At the earliest time possible, the writer (s) is advised whether the article is rejected or accepted.
- b. When an article is accepted and requires revision/modification, the details will be indicated in the return reply from the AJERI Editor, in which case such revision/modification must be completed and returned to AJERI within three months from the date of receipt from the Editorial Staff.
- c. Complementary copies: Following the publishing, three successive issues are sent to the author(s)

Procedure for Submission

- a. Articles for publication must be sent to AJERI on the following address:
The Editor
African Journal of Engineering Research and Innovation
P.O Box 41346- 00100
City Square Nairobi Kenya
Tel: +254 (20) 2729326, 0721 729363, (020) 2716922
E-mail: editor@iekenya.org
- b. The article must bear the writer (s) name, title/designation, office/organization, nationality and complete mailing address. In addition, contributors with e-mail addresses are requested to forward the same to the Editor for faster communication.

For any queries, authors are requested to contact by mail (editor@iekenya.org).

PUBLISHER

The Institution of Engineers of Kenya (IEK)

P.O Box 41346- 00100

City Square Nairobi Kenya

Tel: +254 (20) 2729326, 0721 729363, (020) 2716922

Email: editor@iekenya.org

Website: www.iekenya.org

CONTENTS

Pages

Correlation between material properties and distress features in gravel roads..... 1

F. C. Korir, S. N. Osano, S. K. Mwea

**Evaluation of the Effectiveness of Rice Straw Fibres on Expanded Polystyrene Lightweight Concrete
..... Error! Bookmark not defined.**

W. O. Mocha, S. W. Mumanya, S. O Abuodha

**Improving the municipal solid waste storage system for islands with popular tourist sites and remote
locations using adept storage systems with ventilation systems .. Error! Bookmark not defined.**

J. N. Mativo, M. G. Kim, B. O. Alunda

Wellhead Steam Turbine Retrofit Error! Bookmark not defined.

L. Muloli, P. Chege, C. Maiko, A. Wamwaki

**Informal Settlements challenges implications on the technical solution design for electricity access Error!
Bookmark not defined.1**

O. A. A. Ezzaldeen, A. Muumbo

**Evaluating the Effectiveness of Pumice on Polyvinyl Chloride (PVC)-Treated Red Coffee Soil for Subbase
Construction 69**

C. D. Anyango, M. W. Kibe, J. N. Thuo